https://doi.org/10.5194/egusphere-2026-6398
Preprint. Discussion started: 4 November 2026
© Author(s) 2026. CC BY 4.0 License.

Fully coupled climate–ice-sheet ensemble indicates Greenland Ice Sheet contributed at least one quarter of Last Interglacial sea-level highstand

Christopher J. Larson[1], Matteo Willeit[2], Michael E. Mann[1], Judit Carrillo[3], Annabelle L. Horton[1], Mackenzie M. Weaver[1], and Julia L. Seidenstein[1]

[1]Department of Earth and Environmental Science, University of Pennsylvania, Philadelphia, PA 19104, USA
[2]Potsdam Institute for Climate Impact Research, Potsdam 14412, Germany
[3]Department of Applied Physics, University of La Laguna, La Laguna 38200, Spain

Correspondence: Christopher J. Larson (larsonc@sas.upenn.edu)

Abstract. The Last Interglacial (LIG), or MIS 5e (ca. 130–115 ka), is characterized by high Northern Hemisphere summer insolation and a sea-level highstand about 6–9 m higher than today. The melting of the two polar ice sheets contributed substantially to this sea-level rise but quantifying the contribution from each is difficult. The configuration of the Greenland Ice Sheet (GrIS) during the LIG and its exact contribution to sea level is not well established. Utilizing a fully coupled, fast Earth system model, we ran a 108-member ensemble of coupled climate–GrIS simulations, with a particular focus on the GrIS. We perturbed various ice sheet and geophysical model parameters to create the ensemble, with paleoproxy evidence providing constraints to validate the simulations. The constraints included elevation lowering at the NGRIP, GRIP, GISP2, and NEEM ice core sites from present day to the LIG, the simulated present-day elevation at the GRIP site, and the coverage by ice over all deep Greenland ice core locations throughout the LIG. Only two simulations passed all three primary constraint tests. Relaxing the ice-coverage constraint at Camp Century and Dye-3 results in 13 additional simulations that satisfy the constraints. These simulations result in LIG ice loss of 2.43–3.16 m sea level equivalent, accounting for over a quarter of the LIG sea-level highstand. The remainder of the highstand is unaccounted for by GrIS melt and likely comes from the Antarctic Ice Sheet. Our results demonstrate that the GrIS underwent significant but incomplete retreat during a warm period of elevated insolation, highlighting its potential vulnerability under sustained future anthropogenic greenhouse warming.

1 Introduction

The Greenland Ice Sheet (GrIS, known locally as *Sermersuaq* in the territory of *Kalaallit Nunaat*) contains enough ice to raise global sea level by about 7.4 m if completely melted (Morlighem et al., 2017, 2025). Greenland has mostly or completely deglaciated at least once during the Quaternary (Alley et al., 2010) and Schaefer et al. (2016) show that central Greenland deglaciated at least once in the last 1.1 million years (Myr). These periods of reduced ice volume occurred during interglacial periods, times of relative warmth as revealed by the δ^{18}O in benthic foraminifera (Lisiecki and Raymo, 2005), an indicator of global ice sheet volume and deep ocean temperature.

https://doi.org/10.5194/egusphere-2026-6398
Preprint. Discussion started: 4 November 2026
© Author(s) 2026. CC BY 4.0 License.

Marine Isotope Stage (MIS) 5e (130–115 thousand years ago (ka)), also known as the Last Interglacial (LIG) or the Eemian, is the most recent warmer-than-present interglacial with sea level higher than present and serves as a partial analog for future sea-level rise (Dutton et al., 2015). The LIG is one of the warmest interglacial periods of the past 800 thousand years (kyr) (Otto-Bliesner et al., 2021), characterized by high maximum summer insolation at 65° N. Snyder (2016) estimates global mean surface temperatures approximately 2 °C above pre-industrial levels during the LIG, whereas other proxy reconstructions suggest a warming of about 1 °C (Otto-Bliesner et al., 2013), which is comparable to current-day warmth. These estimates are uncertain due to spatial and temporal sampling uncertainties and potential biases in the proxy data. Models, by contrast with these estimates, show only slight or no warming relative to pre-industrial temperatures (Otto-Bliesner et al., 2021).

Regional high-latitude warmth was nonetheless likely considerably greater than today. Evidence suggests Greenland temperatures peaked between 5 to 8 °C above pre-industrial levels (CAPE-Last Interglacial Project Members, 2006; NEEM community members, 2013). Sea level was likely 6–9 m higher than present (Kopp et al., 2009). Thermal expansion of the ocean only contributed 0.4 $\pm$ 0.3 m at most during the LIG (McKay et al., 2011). Such a rise in sea level thus requires partial to complete deglaciation of the GrIS as well as potentially partial deglaciation of the Antarctic Ice Sheet (AIS). While ice core data suggest that the GrIS survived during the LIG at each ice core location, these data, along with marine records, also suggest a smaller GrIS than present (Holschuh et al., 2026).

The contribution from the GrIS to sea level during the LIG remains uncertain. Various attempts to quantify the contribution of the GrIS to the LIG sea-level highstand have been made using various different models (Cuffey and Marshall, 2000; Tarasov and Peltier, 2003; Calov et al., 2005; Robinson et al., 2011; Helsen et al., 2013; Dendy et al., 2017). These past studies yield a wide range of contributions to LIG sea level from the GrIS, from nearly 0 m to over 5.5 m sea level equivalent (SLE). One of the primary limitations to simulating the GrIS during the LIG is the uncertainty in the initial boundary conditions, including its geometry and climatic history prior to the onset of the interglacial. Continuous proxy reconstructions spanning the preceding glacial period through the LIG would provide stronger constraints on the evolving climate and initial state of the GrIS, allowing for more faithful initialization of the model simulations, and better quantification of the response of the LIG to evolving climatic conditions. One Greenland ice core (NEEM) has continuous temperature and precipitation records throughout the entire LIG; utilizing the proxy estimates from one single ice core in model initialization, however, would already partly prescribe the ice sheet evolution due to the effect of the elevation changes on the inferred surface air temperature. To avoid such biases and complications, coupled climate–ice-sheet model simulations are run to simulate the climate over Greenland using the boundary conditions available (greenhouse gas concentrations and orbital configuration).

A single coupled General Circulation Model (GCM) run through the entire glacial cycle can provide the boundary conditions needed to force an ice sheet model, but doing so requires a considerable amount of computational power. Earth system models of intermediate complexity (EMICs) are computationally efficient enough to run through glacial cycles (Bonelli et al., 2009; Ganopolski et al., 2010; Ganopolski and Brovkin, 2017), even in the context of a large ensemble. EMICs are therefore useful tools to study the co-evolution of climate and ice sheets on millennial to orbital times scales.

The aim of this study is to use a broad but physically plausible range of parameter values important to ice sheet mass loss along with paleo and present-day data to constrain GrIS contribution to the LIG sea-level highstand. We do this uti-

https://doi.org/10.5194/egusphere-2026-6398
Preprint. Discussion started: 4 November 2026
© Author(s) 2026. CC BY 4.0 License.

lizing a newer, state-of-the-art EMIC, CLIMBER-X (Willeit et al., 2022, 2024). CLIMBER-X is a fast EMIC, designed to simulate evolution of the Earth system on time scales from decades to millennia. CLIMBER-X is the successor to the EMIC CLIMBER-2, which has been used to simulate transient glacial-interglacial cycles of the past 3 Myr (Willeit et al., 2019). The primary advantage of this model is that it provides a balance between computational efficiency and process representation while remaining computationally feasible for large ensembles of multi-millennial simulations. Unlike ice sheet models forced by prescribed climate fields, CLIMBER-X simulates two-way interactions between the climate system and the GrIS, allowing the atmosphere, ocean, and ice sheet to evolve interactively.

We performed an ensemble of transient coupled climate-GrIS simulations through the LIG. Only the GrIS was modeled while all other Northern Hemisphere (NH) ice sheets were prescribed; Antarctica was not treated as dynamic in our simulations. We also varied the fraction of meltwater that enters the ocean from the ice sheets to cover the range of possible Atlantic Meridional Overturning Circulation (AMOC) behaviors. Finally, we ran the same ensemble for 30 kyr at constant pre-industrial (1850 CE) boundary conditions (insolation at 65° N = 481 W m^{-2}, CO_2 = 286 ppm, CH_4 = 795 ppb, N_2O = 270 ppb) to obtain the pre-industrial configuration of each simulation (hereafter referred to as the present-day equilibrium simulations), for use against present-day constraints to assist with validating possible GrIS extents.

The framework of this study closely follows that of Robinson et al. (2011), where the authors coupled a simple regional energy balance model to an ice sheet model to identify parameter combinations consistent with LIG observations. We build on this approach by using a fully coupled climate–ice-sheet model and a 108-member ensemble to systematically explore four uncertain model parameters. While retaining the constraints on present-day elevation and LIG elevation lowering at GRIP, we extend the latter to multiple Greenland ice core locations and incorporate additional constraints on ice core coverage. This allows us to identify plausible LIG GrIS configurations and quantify their contributions to sea-level rise.

2 Model description

In this study, we use the fast CLIMBER-X Earth system model (v1.4.0; Willeit et al., 2022). The climate component includes the Semi-Empirical dynamical-Statistical Atmosphere Model SESAM (Willeit et al., 2022), the 3-D frictional-geostrophic ocean model GOLDSTEIN (Edwards et al., 1998; Edwards and Marsh, 2005), the dynamic-thermodynamic sea ice model SISIM (Willeit et al., 2022), and the land surface and dynamic vegetation model PALADYN (Willeit and Ganopolski, 2016), all with a horizontal resolution of 5°x 5°.

SICOPOLIS (Greve, 1997) is used as the ice sheet model for the GrIS at a resolution of 16 km. SICOPOLIS has been used in many NH glaciation studies, especially with the predecessor to CLIMBER-X, CLIMBER-2 (Calov et al., 2005; Ganopolski et al., 2010; Willeit et al., 2019; Carrillo et al., 2024). We use SICOPOLIS v5.3 (SICOPOLIS Authors, 2022), which employs a combination of the hybrid shallow-ice-shelfy-stream dynamics (Bernales et al., 2017), the shallow-ice approximation for grounded non-streaming ice, and the shallow-shelf approximation for floating ice, as well as the enthalpy method for the thermodynamics solver (Greve and Blatter, 2016). SICOPOLIS is run with a Glen's flow law stress exponent of $n = 3$ and a flow enhancement factor of 3.0 for all grounded non-streaming ice. SICOPOLIS is coupled throughout CLIMBER-X via the

https://doi.org/10.5194/egusphere-2026-6398
Preprint. Discussion started: 4 November 2026
© Author(s) 2026. CC BY 4.0 License.

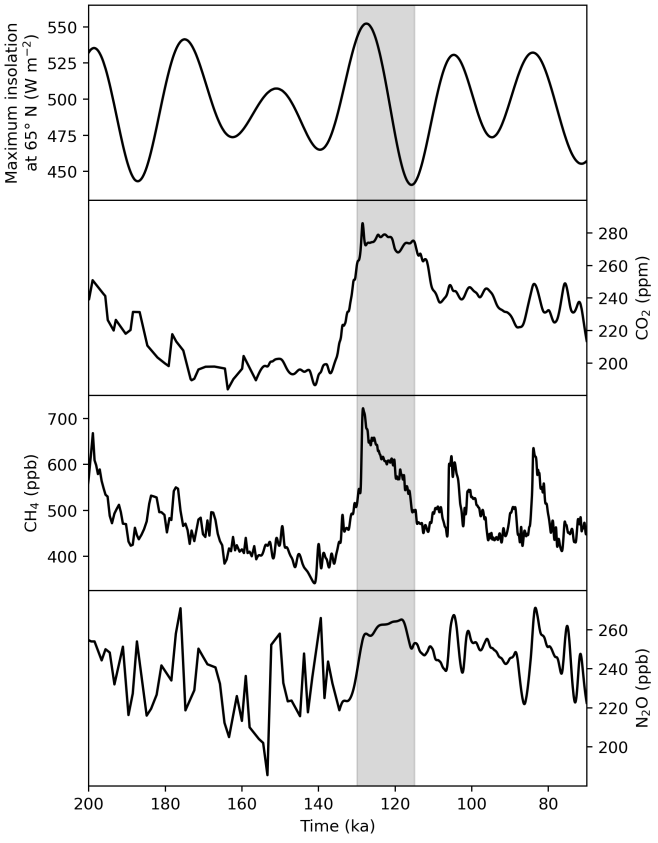


Figure 1. Maximum summer insolation at 65° N (Laskar et al., 2011) and CO_2 (Köhler et al., 2017; Lüthi et al., 2008), CH_4 (Köhler et al., 2017; Loulergue et al., 2008), and N_2O (Köhler et al., 2017; Schilt et al., 2010) from ice cores, used as forcings for the simulations. The Last Interglacial is shaded as 130–115 ka.

physically based surface energy and mass balance interface SEMIX (Willeit et al., 2024; Calov et al., 2005), and the solid Earth model VILMA (Klemann et al., 2008; Martinec et al., 2018) for isostatic uplift and sea level. VILMA in this study is run with a 3D viscosity structure from Bagge et al. (2021). The GrIS is initialized with a uniform ice temperature of -10 °C, following Willeit et al. (2024). Although this initial temperature distribution is not in equilibrium with the climate, the long spin-up period prior to the LIG allows the ice temperature to adjust, minimizing its influence on the simulated LIG evolution. We also include the summer temperature bias correction over North America as seen in Willeit et al. (2024), which has no effect over Greenland. No other bias corrections are applied in this study. More information about the coupling of ice sheets to other CLIMBER-X model components, as well as SICOPOLIS within CLIMBER-X, can be found in Willeit et al. (2024).

https://doi.org/10.5194/egusphere-2026-6398
Preprint. Discussion started: 4 November 2026
© Author(s) 2026. CC BY 4.0 License.

3 Experimental setup

3.1 Transient simulations through the LIG

LIG simulations were run from 200 ka BP, before the preceding glacial period (MIS 6, ca. 190–130 ka), through the LIG, until at least 105 ka BP. Running through the previous glacial period (70 kyr before onset of the LIG in this case) is essential as the ice sheet model runs through an entire glacial period and begins the LIG with a realized ice sheet configuration.

Our focus is on melt of the GrIS during the LIG, so all other NH ice sheets were prescribed in our simulations. All NH ice sheets outside the GrIS were prescribed using the ice sheets from Willeit et al. (2019), modeled using CLIMBER-2 (and SICOPOLIS as the ice sheet model). This previous model did not account for changes in the AIS, and in the study by Willeit et al. (2019), 10 % of the glacial-interglacial sea-level variations were attributed to these changes. The prescribed ice sheet thickness from Willeit et al. (2019) was linearly scaled by a factor of 1.35 to better match the global sea level from Spratt and Lisiecki (2016) during the LIG. A reduction in the prescribed ice thickness over time results in the consequent meltwater being added to the ocean through the steepest surface elevation gradient routing to the ocean. The simulations were forced by changes in orbital configuration (Laskar et al., 2011) and atmospheric greenhouse gas concentrations (CO_2, N_2O, CH_4) from ice cores (Köhler et al., 2017; Lüthi et al., 2008; Schilt et al., 2010; Loulergue et al., 2008) (Fig. 1).

3.2 Parameter ensemble

We perturbed four parameters in our simulations: timescale for ice-discharge parameterization (*tau_dmb*), geothermal heat flux (*q_geo_ice_const*), sliding law coefficient (*c_slide*), and meltwater flux into the ocean (*scale_dhdt_ice*) (Table 1).

These same parameters were used for the present-day equilibrium simulations. In total, each ensemble comprises 108 parameter combinations that span the prescribed parameter space (two ensembles).

3.2.1 Ice-discharge timescale

Albeit a relatively high ice sheet model resolution used in this study, small-scale ice discharge and ice streams cannot be resolved and must therefore be parameterized. Ice sheet dynamical processes may have contributed to LIG ice loss; recent studies of current and future sea-level rise attribute at least some ice sheet mass loss to accelerated dynamical responses (Plach et al., 2019). These processes also depend on the time scales of interest; a higher-resolution ice sheet model makes a greater difference in simulating ice sheet changes on centennial time scales, but not quite as much on longer time scales, such as presented in this study (Aschwanden et al., 2019). It is worth noting that even with a higher ice sheet model resolution, the resolution of the other coupled models (e.g. the ocean model) would also need to increase in order to resolve the dynamics that influence these processes (e.g. fjord circulation for marine-terminating glaciers). SICOPOLIS includes the ice-discharge parameterization for this reason.

The timescale for parameterization of sub-grid ice discharge (*tau_dmb*) in SICOPOLIS is the time in which the ice sheet model parameterizes fast ice discharge through marine outlet glaciers on grids too coarse to resolve individual streams. An

https://doi.org/10.5194/egusphere-2026-6398
Preprint. Discussion started: 4 November 2026
© Author(s) 2026. CC BY 4.0 License.

uncertain and tunable parameter, increasing the timescale for this process allows the ice sheet to grow, where sediment may dominate the bed of the ice sheet (and therefore where outlet glaciers accelerate faster than other regions of the ice sheet). We found the values 20, 30, and 40 years to provide the best match to the current state of the GrIS and therefore the most appropriate for current GrIS dynamics.

3.2.2 Geothermal heat flux

Geothermal heat flux plays an important role in sliding at the base of an ice sheet; if the ice sheet is not frozen to the bed, sliding occurs at the base. The geothermal heat flux below the GrIS is highly uncertain (Zhang et al., 2024) and therefore we set it to a constant value underneath the entire GrIS. The ensemble mean of several modeling studies discussed in Zhang et al. (2024) shows that current understanding of geothermal heat flux at the base of the GrIS is between 50 and 60 mW m^{-2} over most of the island. Lower values can be found in localized spots around 40 to 50 mW m^{-2} in the southwest region of the GrIS and higher values (60 to 70 mW m^{-2}) can be found in the eastern side of the island. Values near the summit of the GrIS are the highest (60 to 80 mW m^{-2}). We tested spatially uniform geothermal heat flux (*q_geo_ice_const*) values of 50, 60, and 70 mW m^{-2} in our simulations.

3.2.3 Sliding law coefficient

The sliding law coefficient represents a poorly constrained parameter governing the sensitivity of ice flow to basal conditions and therefore introduces substantial uncertainty in simulated ice sheet dynamics. Basal sliding is difficult to constrain observationally and is therefore commonly treated as a tunable parameter in ice sheet models, with some approaches using spatially varying sliding coefficients calibrated against observed ice sheet geometry and velocity (e.g., Larour et al., 2012). We include the basal sliding coefficient in our ensemble to assess its influence on simulated ice sheet evolution.

In this study, we use a Weertman-type sliding law:

$$\tau_b = \frac{1}{c_s^{1/p}} N^{q/p} u_b^{1/p}, \tag{1}$$

where $p = 3$ and $q = 2$, τ_b is the basal drag, u_b is the basal velocity, N is the reduced basal pressure if the ice sheet is below sea level, and c_s is the sliding parameter. The sliding parameter depends on the sediment fraction in each grid cell:

$$c_s = (1 - f_{sed}) c_s^{rock} + f_{sed} c_s^{sed}. \tag{2}$$

The sediment fraction is a linear function of sediment thickness between 10 and 500 m (Fig. S1 in the Supplement). The sediment thickness is based on data from Laske et al. (2013). The default value in the model for the sliding coefficient over bedrock is c_s^{rock} = 25 m yr^{-1} Pa^{-1} (from tuning to the present-day GrIS in Calov et al. (2018)). The value for the sliding coefficient over sediment is 10 times this value, c_s^{sed} = 250 m yr^{-1} Pa^{-1}. Sliding over sediment is more crucial at the margins of the GrIS where there is more regolith and therefore more ice discharge, particularly in areas of outlet glaciers. Sliding over bedrock dominates the interior of the GrIS as much of the regolith has been eroded away (Clark and Pollard, 1998) or the Ice Sheet is frozen to the bed (MacGregor et al., 2016) (Fig. S2).

https://doi.org/10.5194/egusphere-2026-6398
Preprint. Discussion started: 4 November 2026
© Author(s) 2026. CC BY 4.0 License.

Parameter	Description	Units	Values
tau_dmb (t)	Timescale for ice-discharge parameterization	yr	20, 30, 40
q_geo_ice_const (q)	Geothermal heat flux for ice sheets	mW m^{-2}	50, 60, 70
c_slide (c)	Basal sliding coefficient over rock	m yr^{-1} Pa^{-1}	10, 50, 100, 150
scale_dhdt_ice (s)	Fraction of melt runoff into ocean	–	0, 0.5, 1

Table 1. Model parameters and corresponding values varied across the simulation ensemble.

In preliminary Last Glacial Maximum (LGM, ca. 20 ka) simulations (with the GrIS at a resolution of 16 km), there was essentially no change in mass loss or gain when increasing the basal sliding coefficient for bedrock (c_s^{rock}) above 150 m yr^{-1} Pa^{-1} (and coincidentally the basal sliding coefficient for sediment (c_s^{sed}) above 1500 m yr^{-1} Pa^{-1}) (Fig. A1). We therefore use values 10, 50, 100, and 150 m yr^{-1} Pa^{-1} for c_s^{rock} for this study. The basal sliding coefficient over bedrock (*c_slide*) is listed in Table 1 whereas the basal sliding coefficient over sediment is not explicitly listed (it is included in these simulations and taken as 10 times these values, i.e. 100, 500, 1000, and 1500 m yr^{-1} Pa^{-1}).

3.2.4 Meltwater flux into ocean

As ice sheets melt and fresh meltwater enters the ocean, the diluted salinity can result in a weakened deep-water formation and consequently a weaker overturning circulation (Bakker et al., 2016). Complete or partial shutdown of AMOC has been theorized during other past deglacial periods, like Heinrich event 1 (H1, about 17.5 ka), when large-scale melt of NH ice sheets introduced ample freshwater into the northern Atlantic (McManus et al., 2004). Changes in AMOC strongly affect climate in the northern North Atlantic region (Zhang et al., 2019; Ma et al., 2024) and therefore also the surface mass balance of the GrIS. In an attempt to explore the impact of the uncertain relation between AMOC and the GrIS, we varied the fraction of melt runoff from the ice sheets (both the interactive GrIS and the other prescribed NH ice sheets) reaching the ocean, using values of 1, 0.5, and 0 (1 meaning all melt runoff enters the ocean and 0 meaning none of the runoff enters the ocean). These values are not intended to represent physically realistic estimates of actual runoff but rather an idealized sensitivity experiment spanning the uncertainty in freshwater–AMOC coupling.

3.3 Present-day equilibrium simulations

The present-day GrIS for each simulation was modeled by running each simulation with the same parameters (i.e. *tau_dmb*, *q_geo_ice_const*, *c_slide*, and *scale_dhdt_ice*) as the LIG simulations and constant pre-industrial (1850 CE) orbital parameters and atmospheric greenhouse gas concentrations for 30 kyr. The AIS is static at its present day state in these simulations while the GrIS evolves dynamically from its present-day configuration. Present day was taken as the final timestep (end) of the simulation, long after reaching steady-state (Fig. S3).

https://doi.org/10.5194/egusphere-2026-6398
Preprint. Discussion started: 4 November 2026
© Author(s) 2026. CC BY 4.0 License.

4 Constraints

Despite evidence for substantial retreat, the extent and geometry of the GrIS at its minimum during the LIG remain poorly constrained. To identify plausible GrIS configurations during the LIG, we will need to abide by a few constraints backed by proxy evidence, with information gathered from Greenland ice cores. The three constraints used in this study are described below.

4.1 LIG elevation lowering from present day

The elevation minimum during the LIG used in this study is the minimum elevation between 130 and 115 ka. Present-day model values in this case were taken as the elevation of each ice core location at the final timestep of the present-day equilibrium simulations. LIG elevation lowering from present day for the Camp Century, Dye-3, and NGRIP locations are not well-constrained. According to NEEM community members (2013), the NEEM ice core is the only Greenland ice core that covers the entire LIG period (and it extends into the preceding glacial period, MIS 6). The authors estimated an elevation decrease of 130 $\pm$ 300 m using insolation-corrected air content. We therefore apply the constraint that the NEEM ice core location minimum LIG elevation was at most 430 m below the simulated present day. Following Robinson et al. (2011), we apply a similar elevation lowering constraint to the summit of the GrIS. The total gas content in the GRIP ice core during the LIG is similar to Holocene levels, with some measurements only slightly higher (Raynaud et al., 1997). The minimum elevation of the GRIP ice core location during the LIG was likely around 300 m below present day, but there is approximately 350 m of uncertainty in this measurement (Cuffey and Marshall, 2000). We therefore apply the constraint that the minimum LIG elevation at the GRIP location is no more than 600 m below the simulated present day. The same constraint was applied to the GISP2 location, due to its proximity to GRIP, as well as the NGRIP location, where elevation lowering is expected to be similar, if not less (North Greenland Ice Core Project members, 2004).

4.2 Simulated present-day GRIP elevation

The elevation at Summit is the most representative of the GrIS as changes in the thickest part of an ice sheet represent the large-scale changes in the surface mass balance without requiring information like the loss of ice at the margins (Alley et al., 2010). Raynaud et al. (1997) found in their model that while the ice margin varied 100–200 km, the elevation change at GRIP remained below 100 m. We therefore implement the constraint that the simulated GRIP location elevation at present day is within $\pm$100 m of the BedMachine Greenland v6 GRIP elevation (3232 m) (Morlighem et al., 2017, 2025).

4.3 Ice core location coverage

Even if most Greenland ice cores do not contain a continuous record through the LIG, these cores still contain a wealth of knowledge before and after this period. Ice dating to the LIG or beyond has been analyzed in the six deep ice cores drilled to the base of the GrIS: Camp Century, Dye-3, GRIP, GISP2, NGRIP, and NEEM (Yau et al., 2016b). Ancient DNA in the silt beneath the Dye-3 ice core predates the LIG (Willerslev et al., 2007), indicating a forested southern Greenland sometime

https://doi.org/10.5194/egusphere-2026-6398
Preprint. Discussion started: 4 November 2026
© Author(s) 2026. CC BY 4.0 License.

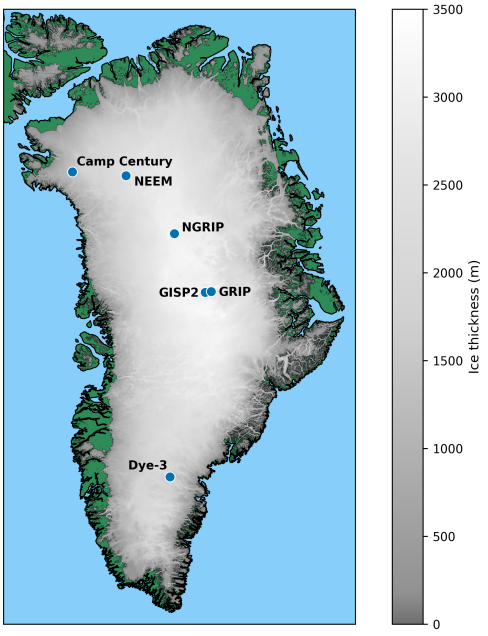


Figure 2. Present-day Greenland Ice Sheet ice thickness from BedMachine Greenland v6 (Morlighem et al., 2017, 2025), with the locations of the six ice cores used to constrain the ensemble indicated by blue circles.

before MIS 11 (ca. 424–374 ka). In addition, a sediment core from the Eirik Drift points toward the retreat of ice from southern Greenland during MIS 11 (Reyes et al., 2014) and not later (i.e. during the LIG). Low δ^{18}O near the bedrock in the NEEM ice core suggests that the ice layers are likely from the glacial period before the LIG. Continuous ice through the LIG also provides potential evidence that the NEEM ice core location was covered throughout this interglacial period (NEEM community members, 2013). Silty ice from the GRIP ice core suggests glacial coverage in central Greenland since about 1 million years ago (Ma) (Yau et al., 2016a). The nearby GISP2 ice core has basal ice with δ^{40}Ar/^{38}Ar ages older than 250 ka (Bender et al., 2010), predating the LIG. The Camp Century ice core in northwestern Greenland contains evidence that the location had at least two ice-free events, one during the Early Pleistocene and one after 1 Ma (Christ et al., 2021). The upper sediment in the Camp Century subglacial core has a luminescence age of 416 $\pm$ 38 ka, indicating the last deglaciation at this location during MIS 11 (Christ et al., 2023). The NGRIP ice core contains a climate record back to 123 ka, and δ^{18}O values indicate that the GrIS at this location did not melt away during the LIG and was only a few hundred meters lower in elevation than today (North Greenland Ice Core Project members, 2004). The final constraint is therefore that all ice core locations remain covered by ice throughout the LIG in our simulations.

https://doi.org/10.5194/egusphere-2026-6398
Preprint. Discussion started: 4 November 2026
© Author(s) 2026. CC BY 4.0 License.

Constraint	Description	Value if true
LIG lowering test	Reduction in elevation at ice core location from present day to LIG minimum	< 600 m for NGRIP, GRIP, and GISP2 < 430 m for NEEM
Summit test	Present-day surface elevation at GRIP	Within ± 100 m of BedMachine Greenland v6 elevation (3232 m)
Ice core location coverage test	Continuous ice coverage at all six ice core locations throughout the LIG	Ice remains present at all six locations throughout the LIG

Table 2. Constraint tests used to evaluate the validity of simulated Greenland Ice Sheet evolution through the Last Interglacial.

5 Results

Simulations in our ensemble that pass the LIG lowering test, the Summit test, and the ice core location coverage test are considered valid (Table 2). We then examine additional cases by first relaxing the ice coverage constraint at Dye-3 and subsequently at Camp Century. GrIS extent during the LIG is uncertain but we expect all ice core sites to remain covered, with melt focused on the margin of the GrIS. Modeling studies such as that presented here can help constrain the spatial extent and configuration of the GrIS during the LIG.

5.1 Constraint tests

The parameters in the ensemble produced 108 individual simulations (Fig. 3). The entire ensemble resulted in a sea-level contribution between 2.23 and 5.21 m during the LIG from the GrIS, with an average contribution of 3.42 ± 0.73 m SLE (Fig. S4).

Of the 108 simulations, 37 passed the LIG lowering test. The simulations that passed the LIG lowering test contributed between 2.23 and 3.32 m to LIG sea level, with an average of 2.70 ± 0.28 m SLE. This is equivalent to an average minimum LIG GrIS 35 % smaller than their associated present-day simulations.

A total of 25 simulations passed the Summit test. The simulations that passed the Summit test contributed between 2.43 and 4.13 m to LIG sea level, with an average of 3.15 ± 0.57 m SLE. This is equivalent to an average minimum LIG GrIS 42 % smaller than their associated present-day simulations.

The ice core location coverage test was satisfied by four simulations. The simulations that passed the ice core location coverage test contributed between 2.23 and 2.56 m to LIG sea level, with an average of 2.40 ± 0.13 m SLE. This is equivalent to an average minimum LIG GrIS 29 % smaller than their associated present-day simulations.

The margin of the GrIS is the first to melt, likely due to faster ice discharge, enhanced basal melting caused by frictional flow, or warmer temperatures at lower altitudes (Robinson et al., 2012), or a combination of these. Dye-3 sits on a southern dome, in a region of relatively thicker ice, but it often became deglaciated in our simulations. The ice core location coverage test

https://doi.org/10.5194/egusphere-2026-6398
Preprint. Discussion started: 4 November 2026
© Author(s) 2026. CC BY 4.0 License.

was the most difficult to pass; continuous ice coverage over every ice core location proved very challenging in our simulations due to the marginal locations of Camp Century and Dye-3. The runs that passed the ice core location coverage test are runs c10_t40_q50_s1 (c_slide = 10 m yr^{-1} Pa^{-1}, tau_dmb = 40 yr, $q_geo_ice_const$ = 50 mW m^{-2}, and $scale_dhdt_ice$ = 1), c10_t40_q50_s0.5, c10_t40_q60_s1, and c50_t40_q50_s0.5. Runs c10_t40_q50_s1 and c10_t40_q50_s0.5 are very similar in that they only differ in meltwater flux.

5.2 "Best" simulations

Only two simulations passed all three tests. These two "best" simulations are c10_t40_q60_s1 and c50_t40_q50_s0.5 (Table 3). While c10_t40_q50_s1 and c10_t40_q50_s0.5 pass the ice core location coverage test, these simulations fail the Summit test. Using the present-day GrIS simulated in their corresponding present-day equilibrium simulations, c10_t40_q60_s1 and c50_t40_q50_s0.5 result in a minimum LIG GrIS 30 % and 32 % smaller, respectively, than present day (Fig. 4). The sea-level contribution from the GrIS during the LIG for these simulations is 2.43 and 2.56 m, respectively.

CLIMBER-X exhibits some biases in the simulated present-day climate, in particular the regional precipitation over Greenland. There is not enough precipitation at present in northwestern Greenland, making the GrIS particularly susceptible to retreat in that region. The Camp Century location, therefore, might too easily become uncovered by the ice during the LIG. The model also underestimates precipitation in southeastern Greenland, possibly resulting in the lack of ice coverage at the Dye-3 location. Additionally, some modeling studies indicate that Dye-3 became ice-free during the LIG (Tarasov and Peltier, 2003; Lhomme et al., 2005; Robinson et al., 2011), an interpretation consistent with the absence of a preserved LIG record in the Dye-3 ice core (Willerslev et al., 2007). Consistent with these previous studies, Dye-3 becomes ice-free during the LIG in an overwhelming majority of our simulations (Fig. 5).

We therefore present two additional cases of "best" simulations: (i) Camp Century covered by ice but not Dye-3 during the LIG (Dye-3 coverage during the LIG disputed) and (ii) Camp Century and Dye-3 (or either) uncovered by ice during the LIG (considering the first case and the model biases). In the first case, if we were to relax ice core location coverage at the Dye-3 location, this would add three more simulations into the "best" category (five total), passing the other two tests. These three simulations have the same parameter values as the original two "best" simulations, except for the meltwater flux (i.e. c_slide = 10 or 50 m yr^{-1} Pa^{-1}, tau_dmb = 40 yr, $q_geo_ice_const$ = 50 or 60 mW m^{-2}, and $scale_dhdt_ice$ = 0, 0.5, or 1). These additional simulations result in an average 2.52 $\pm$ 0.12 m (2.43–2.73 m) contributed to LIG sea level. These result in an average minimum LIG GrIS 32 % smaller than present day.

In the second case, if we were to relax the ice core location coverage by ice at both the Camp Century and Dye-3 locations, this would add 10 more simulations into the "best" category (15 total), as shown in Table 3. These additional simulations result in an average 2.65 $\pm$ 0.22 m (2.43–3.16 m) contributed to LIG sea level. These equate to an average minimum LIG GrIS 33 % smaller than present day. The simulated present-day ice sheet configurations for the 15 accepted simulations across all three cases are shown in Fig. A2.

https://doi.org/10.5194/egusphere-2026-6398
Preprint. Discussion started: 4 November 2026
© Author(s) 2026. CC BY 4.0 License.

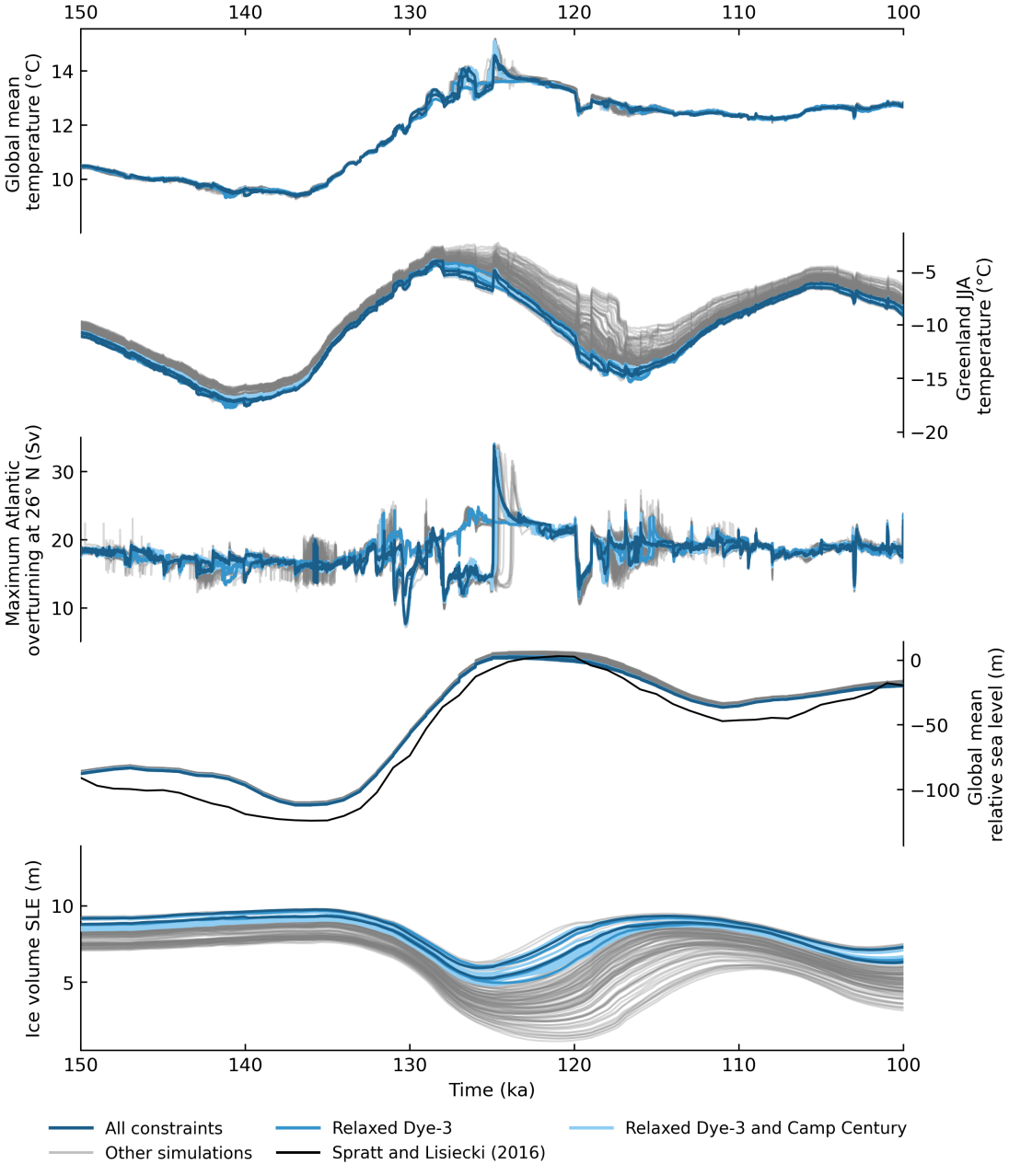


Figure 3. Simulated evolution of global mean near-surface air temperature, mean summer near-surface air temperature over Greenland, AMOC, global mean relative sea level, and Greenland Ice Sheet volume (m SLE) from 150 to 100 ka for the full ensemble (gray lines). Dark blue lines indicate the two simulations satisfying all constraints, medium blue lines indicate the three additional simulations accepted when the Dye-3 constraint is relaxed, and light blue lines indicate the 10 additional simulations accepted when both the Dye-3 and Camp Century constraints are relaxed. The black line indicates the global mean relative sea level from Spratt and Lisiecki (2016).

https://doi.org/10.5194/egusphere-2026-6398
Preprint. Discussion started: 4 November 2026
© Author(s) 2026. CC BY 4.0 License.

Case	Simulations		
All constraints	c10_t40_q60_s1 c50_t40_q50_s0.5		
Relaxed Dye-3	c10_t40_q60_s0 c10_t40_q60_s1	c50_t40_q50_s0 c50_t40_q50_s0.5	c50_t40_q50_s1
Relaxed Dye-3 and Camp Century	c10_t30_q50_s0 c10_t30_q50_s0.5 c10_t30_q50_s1 c10_t30_q60_s0 c10_t30_q60_s0.5	c10_t30_q60_s1 c10_t30_q70_s0.5 c10_t30_q70_s1 c10_t40_q60_s0 c10_t40_q60_s0.5	c10_t40_q60_s1 c10_t40_q70_s0.5 c50_t40_q50_s0 c50_t40_q50_s0.5 c50_t40_q50_s1

Table 3. "Best" simulations that satisfy all three constraint tests under each ice core coverage criterion.

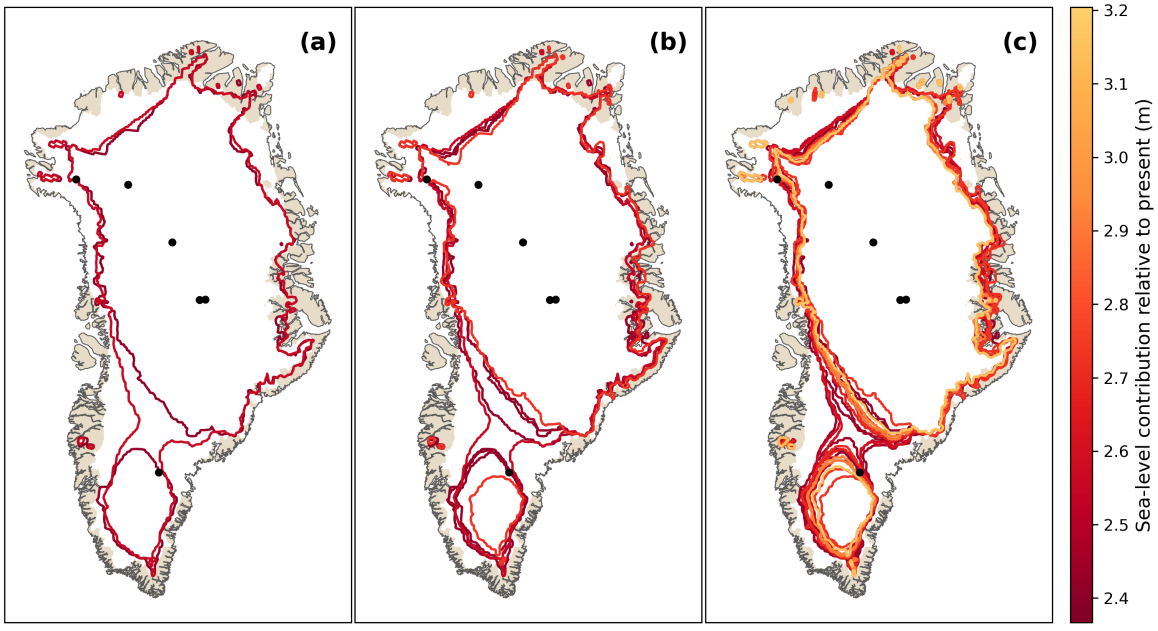


Figure 4. Present-day Greenland Ice Sheet overlain by the minimum ice sheet margin during the Last Interglacial (130–115 ka) for (a) the two "best" simulations that pass all three constraint tests (b) the five simulations that pass all three constraint tests if the Dye-3 constraint is relaxed and (c) the 15 simulations that pass all three constraint tests if the Dye-3 and Camp Century constraints are relaxed. The color of each margin relates to the amount of ice volume SLE contributed to sea level relative to the corresponding present-day equilibrium simulation. Ice core locations are denoted by the black dots.

https://doi.org/10.5194/egusphere-2026-6398
Preprint. Discussion started: 4 November 2026
© Author(s) 2026. CC BY 4.0 License.

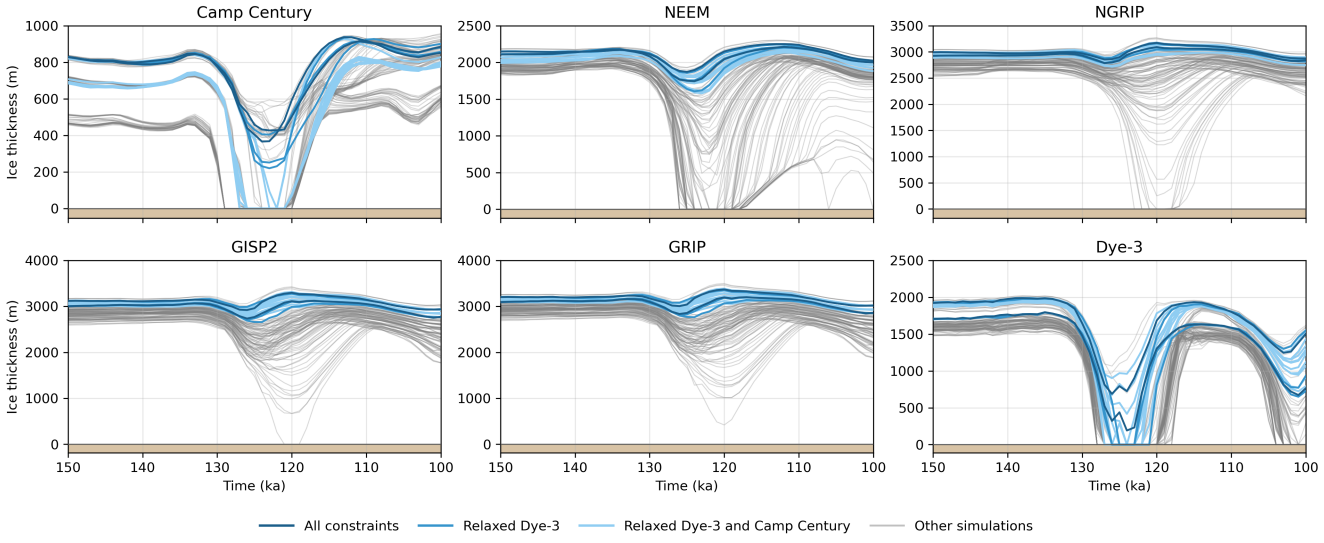


Figure 5. Ice thickness at each ice core location from 150–100 ka for the full ensemble (gray lines). Dark blue lines indicate the two simulations satisfying all constraints, medium blue lines indicate the three additional simulations accepted when the Dye-3 constraint is relaxed, and light blue lines indicate the 10 additional simulations accepted when both the Dye-3 and Camp Century constraints are relaxed. An ice thickness of zero indicates complete local deglaciation. Beige shading represents bare ground.

5.3 Ice sheet thinning

Despite substantial variability in simulated ice thickness among ensemble members, the timing of maximum thinning at each ice core location is consistent across Greenland, occurring between 126 and 121 ka (Fig. 5). Complete loss of the central dome (GRIP, GISP2, and NGRIP) is uncommon, and GRIP is the only ice core location that does not completely melt away in any simulation. The Dye-3 location reaches a minimum during the LIG, and then again across many simulations closer to 100 ka; southern Greenland seems to be particularly susceptible to ice sheet retreat in our simulations. Marginal locations (Camp Century, NEEM, and Dye-3) lose ice in many simulations, and they show much larger amplitude changes. This is consistent with an ice sheet whose margins retreat substantially while the central dome remains comparatively resilient. This behavior is reflected in the three cases of "best" simulations, in which minimum ice sheet extent remains consistently confined to the central and southern domes of the GrIS despite substantial retreat of the ice margins (Fig. 4). Despite differences in the magnitude of ice sheet retreat, all accepted simulations (15 simulations) reach their minimum LIG ice sheet extent between 126 and 124 ka. Among the accepted simulations, mean maximum thinning relative to the corresponding present-day equilibrium simulations ranges from about 217 to 260 m at the central ice core locations (NGRIP, GISP2, and GRIP), compared with 382 m at NEEM, 638 m at Camp Century, and 1523 m at Dye-3. Minimum ice thickness generally occurs between 127 and 123 ka, with the central ice core locations tending to reach their minima earlier than the marginal sites.

https://doi.org/10.5194/egusphere-2026-6398
Preprint. Discussion started: 4 November 2026
© Author(s) 2026. CC BY 4.0 License.

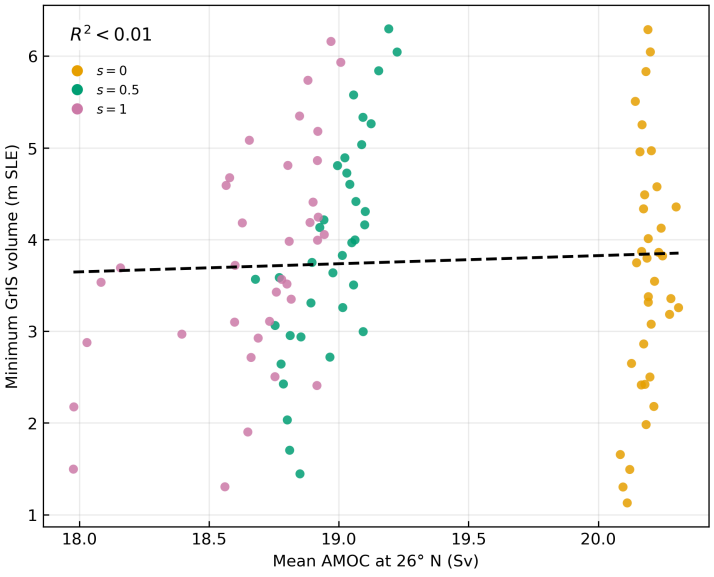


Figure 6. Relationship between mean AMOC strength at 26° N and minimum Greenland Ice Sheet volume during the Last Interglacial (130–115 ka) for the full ensemble. The dashed line represents the linear regression across all simulations, with the corresponding R^2 shown in the upper-left corner. The colors correspond to the meltwater flux value.

5.4 AMOC

Although it has been posited that AMOC weakened or shut down during the LIG (McManus et al., 2004; Böning et al., 2016), AMOC never completely shut down during any of our 108 simulations (Fig. 3), reaching minimum strengths of about 10 Sv. There is, however, a clear AMOC signal during the LIG. In most simulations, AMOC seems to weaken at the climatic optimum of the LIG (around 128 ka) by about 10 Sv. A relatively abrupt weakening of this same magnitude occurs for all simulations around 120 ka, followed by a recovery.

Grouping the ensemble by the meltwater flux reveals three distinct AMOC regimes, despite little relationship between mean AMOC strength and minimum LIG GrIS volume (Fig. 6). A meltwater flux of 0 results in the highest mean AMOC strength (around 20.2 Sv) during the LIG. A fraction of 0.5 results in moderate mean AMOC strength, and a fraction of 1 results in the lowest mean AMOC strength. Despite the strong sensitivity of AMOC strength to meltwater input, ocean overturning alone does not explain the spread in minimum LIG GrIS volume. This is largely because AMOC changes have a more pronounced impact on winter climate over Greenland; GrIS retreat is primarily driven by summer melt, which is less sensitive to AMOC variability and more strongly influenced by local insolation.

https://doi.org/10.5194/egusphere-2026-6398
Preprint. Discussion started: 4 November 2026
© Author(s) 2026. CC BY 4.0 License.

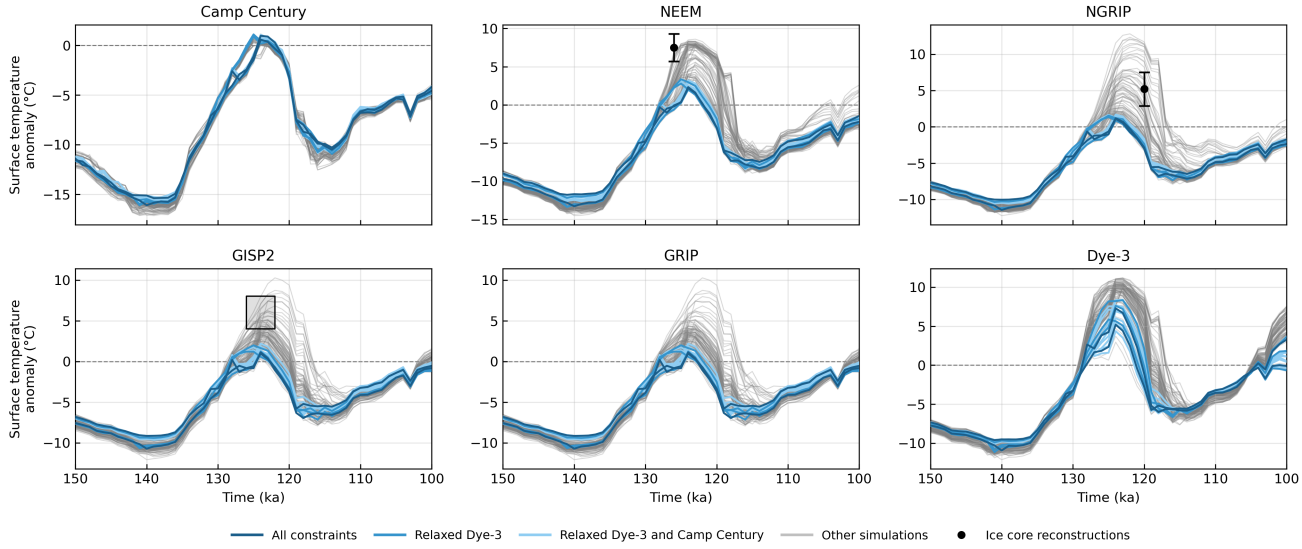


Figure 7. Surface temperature anomalies at each ice core location from 150–110 ka for the full ensemble (gray lines), relative to the corresponding simulated present-day temperatures. Dark blue lines indicate the 2 simulations satisfying all constraints, medium blue lines indicate the 3 additional simulations accepted when the Dye-3 constraint is relaxed, and light blue lines indicate the 10 additional simulations accepted when both the Dye-3 and Camp Century constraints are relaxed. Anomalies are calculated from the annual grid-cell mean 2-m air temperature relative to the final annual mean temperature of the corresponding present-day simulation. Black markers indicate reconstructed Last Interglacial temperature anomalies at NEEM (7.5 ± 1.8 °C at 126 ka; NEEM community members, 2013) and NGRIP (5.2 ± 2.3 °C at 120 ka; Landais et al., 2016). The black rectangle at GISP2 represents reconstructed warming of 4–8 °C between 126 and 122 ka (Yau et al., 2016b). The NEEM reconstruction represents the upstream deposition location rather than the present-day ice core site. GISP2 and GRIP occupy the same atmospheric model grid cell.

5.5 Modeled temperature

Global mean temperature during the LIG in our ensemble varies by about 0.2 °C (13.06 to 13.28 °C), while mean Greenland summer (June-July-August) temperature varies by about 4 °C (-9.5 to -5.5 °C) (Fig. 3). This variability is also evident in modeled surface temperature anomalies at individual ice core sites (Fig. 7). The ensemble spread in temperature anomaly increases substantially during 126–120 ka, coincident with peak LIG warming and ice thinning. Dye-3, NEEM, and NGRIP exhibit particularly large divergence among simulations, while the accepted simulations at Dye-3 show the strongest warming response, reaching roughly +10 °C. Simulated temperatures are more tightly clustered before and after this interval, with relatively little ensemble spread at Camp Century throughout the simulation. The accepted simulations generally exhibit a narrower range of LIG temperature anomalies than the full ensemble, particularly at the central Greenland ice core sites.

Proxy-derived temperature estimates provide additional constraints on the magnitude of this regional warming where available. At NGRIP, where the ice core record extends to 123 ka, Landais et al. (2016) estimate warming of +5.2 ± 2.3 °C relative

https://doi.org/10.5194/egusphere-2026-6398
Preprint. Discussion started: 4 November 2026
© Author(s) 2026. CC BY 4.0 License.

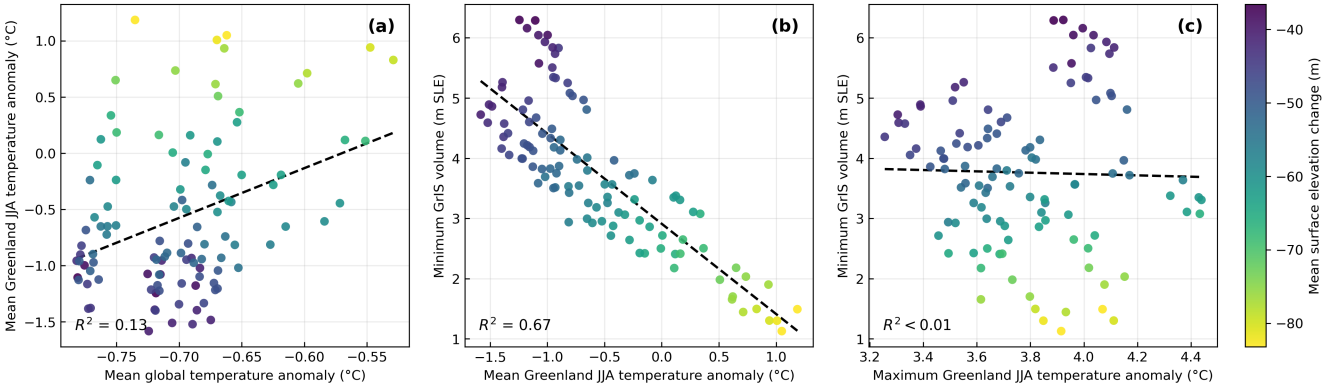


Figure 8. Relationship between (a) mean global temperature anomaly and mean Greenland summer temperature anomaly, (b) mean Greenland summer temperature anomaly and minimum GrIS volume, and (c) maximum Greenland summer temperature anomaly and minimum GrIS volume, for the entire ensemble for the Last Interglacial (130–115 ka). Temperature anomalies are calculated relative to the final 1 kyr mean of the corresponding present-day simulation for each ensemble member. Panels (a) and (b) show mean temperature anomalies over the Last Interglacial, while (c) shows the maximum Greenland summer temperature anomaly during the Last Interglacial. The colors correspond to the mean surface elevation change, calculated as the Last Interglacial surface elevation at minimum Last Interglacial ice volume minus the present-day surface elevation, averaged over the present-day ice-covered area. The dashed line represents the linear regression across all simulations, with the corresponding R^2 shown in the bottom-left corner of the panel.

to pre-industrial at 120 ka. The NGRIP record does not extend through peak LIG warmth, and therefore this estimate may underestimate maximum LIG warming. At NEEM, water isotope measurements indicate warming of +7.5 ± 1.8 °C relative to pre-industrial at 126 ka at the inferred upstream deposition location (NEEM community members, 2013). At Summit, GISP2 records indicate temperatures approximately 4–8 °C warmer than present day between 126 and 122 ka (Yau et al., 2016b). These estimates are not directly comparable to modeled annual mean surface temperature anomalies due to differences in proxy interpretation, seasonality, spatial representation, and age constraints.

The relationship between mean global temperature change from simulated present day to the LIG, mean Greenland summer temperature change, maximum Greenland summer temperature change, and minimum LIG GrIS volume is shown in Fig. 8. Global annual temperature anomaly occupies an extremely narrow range of about -0.8 to -0.5 °C and explains little of the mean Greenland summer spread (R^2 = 0.13). The simulations with the warmest Greenland summers tend to have the largest surface elevation lowering from present day, even when the range of global temperature anomaly is small. Mean Greenland summer temperature anomaly spans nearly 3 °C, and the anomaly has a strong relationship with minimum GrIS volume (R^2 = 0.67), with simulations exhibiting greater ice loss characterized by higher mean surface elevation reduction. Peak Greenland summer temperature has essentially no relationship with minimum GrIS volume ($R^2 < 0.01$), but the ensemble members remain strongly organized by surface elevation lowering. Simulations with a lower minimum GrIS volume exhibit more elevation lowering during the LIG, while simulations with a higher minimum GrIS volume exhibit less elevation lowering, regardless of their maximum summer temperature anomaly.

https://doi.org/10.5194/egusphere-2026-6398
Preprint. Discussion started: 4 November 2026
© Author(s) 2026. CC BY 4.0 License.

Parameter	Δ GMT (°C)	Δ Greenland JJA (°C)	Δ minimum GrIS (m SLE)
Basal sliding coefficient (c)	0.03	1.39	1.77
Ice-discharge timescale (t)	0.04	**1.79**	**2.19**
Geothermal heat flux (q)	0.02	0.90	1.01
Meltwater flux (s)	**0.11**	0.34	0.32

Table 4. Range in simulated climate and Greenland Ice Sheet response associated with each perturbed parameter during the Last Interglacial (130–115 ka). Differences are calculated between the highest and lowest parameter values, with the largest ranges shown in bold.

Table 4 shows the range in simulated climate and minimum GrIS volume during the LIG for each parameter. The meltwater flux has the largest effect on global mean temperature. The ice-discharge timescale has the largest effect on Greenland summer temperature and minimum GrIS volume. Mean global temperature varies little across parameter values, wheres Greenland summer temperatures and minimum GrIS volume exhibit substantially greater sensitivity (Table S1).

6 Discussion

Earlier modeling studies generally produced relatively large GrIS contributions to LIG sea level, ranging from approximately 2.7 to 5.5 m (Cuffey and Marshall, 2000; Huybrechts, 2002; Tarasov and Peltier, 2003; Lhomme et al., 2005). These simulations showed extensive retreat in southeastern Greenland, including loss of ice near Dye-3. Later studies driven by GCM-derived climate anomalies generally retained more ice in southeastern Greenland and produced a broader but lower range of approximately 0.4–4.4 m contributed to LIG sea level (Robinson et al., 2011; Quiquet et al., 2013; Stone et al., 2013).

Coupled climate–ice-sheet simulations have generally produced intermediate estimates, although the results remain strongly dependent on the complexity of the coupling and the represented feedbacks. Helsen et al. (2013) yielded a LIG GrIS contribution of 1.2–3.5 m using a regional atmosphere–ice-sheet coupling. Using the fully coupled EMIC LOVECLIM, Goelzer et al. (2016) simulated a peak GrIS contribution of approximately 1.4 m. Sommers et al. (2021) used the GCM CESM2 coupled with the ice sheet model CISM2 and produced a GrIS contribution of about 3.0 m. A fully coupled simulation of the penultimate termination by Quiquet and Roche (2024) using the EMIC iLOVECLIM produced a GrIS contribution of about 2 m during the LIG. A study by Plach et al. (2019) obtained contributions ranging from approximately 0.5 to 3.0 m using the same regional climate forcing over Greenland but different surface mass balance formulations. Collectively, these studies highlight the substantial model dependence of LIG GrIS sea-level estimates, even when interactions between the climate and ice sheets are represented. Our constraint-based ensemble further narrows this range by identifying GrIS configurations consistent with both LIG paleo-constraints and the simulated present-day state.

https://doi.org/10.5194/egusphere-2026-6398
Preprint. Discussion started: 4 November 2026
© Author(s) 2026. CC BY 4.0 License.

Despite relaxing the ice core constraints, the simulated geometry of minimum LIG GrIS extent changes relatively little, suggesting that the broad spatial pattern of retreat is a robust feature of the ensemble. All 15 accepted simulations retain substantial ice at NGRIP, GISP2, and GRIP, despite considerably greater ice sheet thinning and frequent local deglaciation at the Camp Century and Dye-3 locations. Similarly, the timing of maximum thinning and minimum ice sheet extent is remarkably consistent across the accepted simulations despite substantial differences in the magnitude of ice loss. This suggests that the timing of transient GrIS evolution is relatively insensitive to the model parameters varied here and more closely follows the common large-scale LIG climate forcing, whereas these parameters exert a stronger influence on the magnitude of ice sheet retreat.

Reconstructions of LIG ice thickness are sparse. At NEEM, ice sheet thinning of approximately 400 $\pm$ 250 m between 128 and 122 ka has been reconstructed (NEEM community members, 2013). This estimate provides a distinct comparison from the surface elevation constraint used to select the accepted simulations, which is based on minimum LIG elevation relative to the simulated present day. Over the same interval, all accepted simulations produce a mean thinning at NEEM of 113 $\pm$ 98 m (-24 to 257 m). Although six of the 15 accepted simulations fall within the uncertainty range of the reconstruction (150 to 650 m), the accepted ensemble generally produces substantially less thinning than the central estimate of 400 m. More broadly, the persistence of substantial ice thickness at Summit in the accepted simulations is consistent with the survival of a central Greenland ice dome during the LIG. At the more marginal sites, frequent local deglaciation highlights the substantially greater sensitivity of the northern and southern ice sheet margins.

The response of the GrIS to freshwater forcing also provides insight into the role of ocean–ice-sheet feedbacks. Luo et al. (2018) used an Earth system model to show AMOC strength is only slightly reduced during the LIG (from around 125 to 115 ka). This is reinforced by the benthic δ^{13}C from the North Atlantic, which decreased quickly during 127 to 125 ka and then slowly increased at 115 ka (Galaasen et al., 2014). These suggest that AMOC was strong and persistent throughout the LIG. The maximum AMOC strength change in the ensemble mean during the LIG (127 ka) in Jiang et al. (2023) never exceeds 1.5 Sv. Individual simulations in Luo et al. (2018) remain below 2.5 Sv throughout the LIG. In comparison, most of our simulations exhibit AMOC weakening of 10 Sv.

Depending on how quickly Greenland loses mass and therefore the amount and rate of freshwater flux into the North Atlantic, AMOC weakens to varying degrees (this is reflected by the three regimes in Fig. 6). The reduced northward ocean heat transport cools the North Atlantic, which can partially offset Greenland warming. If AMOC weakens substantially, southeast Greenland may cool, snowfall can increase in some regions, and the duration of peak melt may shorten (Wunderling et al., 2024). Across the 108-member ensemble, mean AMOC strength during the LIG explains essentially none of the variance in minimum GrIS volume ($R^2 < 0.01$), suggesting that differences in mean AMOC strength are not a primary control on simulated GrIS retreat. Different mean AMOC states, however, produce very similar ranges of GrIS retreat. This suggests that the AMOC response is dominated by the melting of the other NH ice sheets rather than the GrIS. Further investigation of the ocean model and its parameterizations would be required to better characterize the role of AMOC during the LIG but such is beyond the scope of this study.

https://doi.org/10.5194/egusphere-2026-6398
Preprint. Discussion started: 4 November 2026
© Author(s) 2026. CC BY 4.0 License.

Some simulations within the full ensemble produce local surface temperature anomalies comparable to published LIG temperature reconstructions; however, the accepted simulations generally exhibit less warming than indicated by the reconstructions. This difference cannot be explained solely by differences in the timing of peak warming: across the 130–115 ka interval, the mean maximum annual surface temperature anomaly attained in all 15 accepted simulations is 2.62 ± 0.46 °C at NEEM, 1.31 ± 0.24 °C at NGRIP, and 1.38 ± 0.41 °C at GISP2. By comparison, substantially greater warming occurs at Dye-3 (6.83 ± 1.16 °C), indicating pronounced spatial heterogeneity in the simulated Greenland temperature response. Since the ensemble is being constrained using ice sheet elevation and coverage rather than temperature, the narrower temperature range of the accepted simulations highlights the coupling between simulated ice sheet evolution and the regional surface climate. Direct comparison with the ice core estimates should nevertheless be interpreted cautiously as the proxy-derived temperatures and modeled annual mean grid-cell temperatures differ in their spatial and seasonal representation and sensitivity to changes in ice sheet elevation.

The magnitude of GrIS retreat is much more closely related to Greenland summer climate than global mean temperature, as reflected in the substantially greater spread in Greenland summer temperature across the ensemble (Fig. 8). GrIS melt is also more strongly associated with sustained summer conditions over the LIG than with the magnitude of peak summer warmth, regardless of whether peak warmth is represented by a single maximum or a 1 kyr mean. A similar importance of sustained interglacial warmth has been demonstrated for MIS 11, when the extended duration of warm conditions contributed to substantial GrIS melt (Robinson et al., 2017).

Warmer mean Greenland summers covary with smaller GrIS volumes and greater surface elevation lowering across the ensemble. The relationship between mean Greenland summer temperature and minimum GrIS volume ($R^2 = 0.67$) is substantially stronger than that between maximum summer temperature and minimum GrIS volume, which shows little relationship ($R^2 < 0.01$). Together, the covariance between Greenland summer temperature, GrIS volume, and surface elevation is consistent with a surface-elevation–temperature feedback: as the ice sheet surface lowers through melting, it is exposed to warmer temperatures, which can enhance melt and further lower the surface. This feedback may also contribute to the much larger ensemble spread in mean Greenland summer temperature anomaly (about 3 °C) compared with global mean temperature anomaly (about 0.2 °C).

7 Conclusions

We constrained a transient ensemble of coupled climate–GrIS simulations using paleoproxy evidence to identify plausible LIG ice sheet configurations. Of the 108 simulations, two satisfy all observational constraints: LIG elevation lowering, Summit elevation within ±100 m of present day, and ice core location coverage throughout. This number increases to five when the Dye-3 constraint is relaxed and to 15 when both the Dye-3 and Camp Century constraints are relaxed. Taken together, these constraint-consistent simulations indicate a GrIS contribution to LIG sea level of 2.43–3.16 m. Across these simulations, substantial retreat occurs primarily along the ice sheet margins while a central Greenland ice dome persists. A LIG sea-level

https://doi.org/10.5194/egusphere-2026-6398
Preprint. Discussion started: 4 November 2026
© Author(s) 2026. CC BY 4.0 License.

highstand of about 6–9 m above present suggests that at least 2.8 m is unaccounted for from GrIS melt, with the majority of the remaining contribution likely coming from the AIS.

The LIG provides an important test of ice sheet sensitivity during a warm period, particularly over millennial timescales that cannot be evaluated using the instrumental record alone. The LIG should not be viewed as a direct analog for the future GrIS because its warming was driven largely by orbital forcing and therefore differed both spatially and seasonally from anthropogenic greenhouse-gas-driven warming. Nevertheless, the LIG provides important evidence detailing how sustained regional summer warmth can produce multi-meter reductions in GrIS volume, informing more generally our understanding of how the GrIS can respond to radiative forcing changes.

As coupled climate–ice-sheet models continue to improve, paleoclimate constraints from the LIG will remain an essential benchmark for reducing uncertainty in projections of GrIS melt. Continued refinements of model parameterizations and the representation of climate–ice-sheet feedbacks, evaluated against paleoclimatic evidence from the LIG, can help constrain model behavior and increase confidence in projections of the long-term GrIS contribution to future sea-level rise.

https://doi.org/10.5194/egusphere-2026-6398
Preprint. Discussion started: 4 November 2026
© Author(s) 2026. CC BY 4.0 License.

Appendix A: Parameter sensitivity analysis

We performed a global sensitivity analysis across all 108 LIG simulations using a four-factor full-factorial design. Parameter importance was quantified by decomposing the ensemble variance into main effects and interactions.

Single-parameter sensitivity of minimum GrIS volume between 150-100 ka (Fig. A3) shows a decreasing trend in minimum GrIS volume with an increasing basal sliding coefficient, which is expected as sliding becomes faster and the GrIS loses mass. The mean response of minimum GrIS volume ranges by about 1.86 m SLE between c_s^{rock} = 10 m yr^{-1} and c_s^{rock} = 150 m yr^{-1}. Geothermal heat flux shares a similar trend with minimum GrIS volume decreasing as the value increases from 50 mW m^{-2} to 70 mW m^{-2}, and a mean change of about 0.95 m SLE. This is also expected, as a higher geothermal heat flux enables more of the basal ice to be at pressure melting point and allow sliding. The ice-discharge timescale produces the only increasing trend, with increasing timescales increasing the minimum GrIS volume. This trend is also the strongest, with mean values increasing about 2.13 m SLE as the timescale increases from 20 years to 40 years. Increasing the timescale increases the amount of time between parameterization of ice discharge from the GrIS, thereby allowing more time for accumulation and increasing the amount of ice present at the margins. The meltwater flux has the least effect on minimum GrIS volume, showing almost no trend (with a mean change of around 0.38 m SLE as the fraction increases). Viewing all of these trends through time for each parameter, there is no significant change in the timing of minimum LIG GrIS volume (Fig. S5).

Variance decomposition of each tested parameter (Fig. S6) reveals that the ice-discharge timescale has the dominant effect on the spread of minimum LIG GrIS volume across the 108-member ensemble during 150–100 ka. The ice-discharge timescale explains over half (51 %) of the variability in GrIS ice mass loss between 150–100 ka; basal sliding explains about 33 %, geothermal heat flux explains about 10 %, and the meltwater flux explains about 2 %.

Each of the four parameters together explain 94.9 % of the total variation among the 108 simulations. All interaction effects explain 5.1 %: two-way interactions explain 2.9 %, three-way interactions 1.4 %, and the four-way interaction 0.8 %. The strongest two-way interaction is between basal sliding and ice-discharge timescale, explaining 1.01 % of the total variation (Fig. A4).

https://doi.org/10.5194/egusphere-2026-6398
Preprint. Discussion started: 4 November 2026
© Author(s) 2026. CC BY 4.0 License.

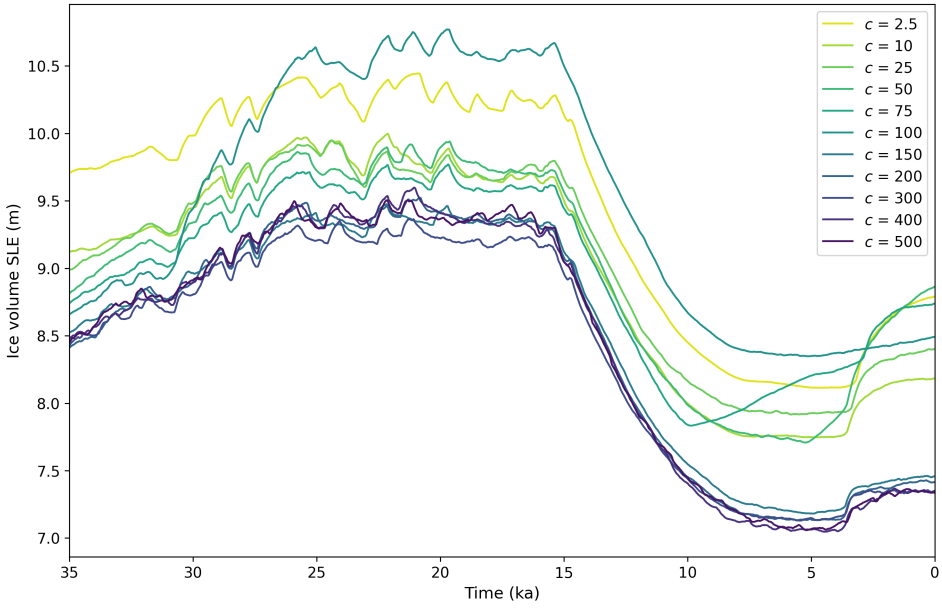


Figure A1. Greenland Ice Sheet volume during the Last Glacial Maximum when varying basal sliding coefficient over bedrock (c_slide). Values 2.5 to 150 m yr^{-1} Pa^{-1} result in independent ice volume evolution over the Last Glacial Maximum. Values above 150 m yr^{-1} Pa^{-1} collapse into the same curve. The mean square error values between c_slide = 150 m yr^{-1} Pa^{-1} and all c_slide values above it range between 4.40×10^{-3} and 1.25×10^{-2} m.

https://doi.org/10.5194/egusphere-2026-6398
Preprint. Discussion started: 4 November 2026
© Author(s) 2026. CC BY 4.0 License.



Figure A2. Greenland Ice Sheet thickness for the present-day equilibrium simulations corresponding to each simulation that satisfied the constraints. Colored contours indicate the simulated present-day ice sheet margins: satisfies all constraints (dark blue), relaxed Dye-3 (medium blue), and relaxed Dye-3 and Camp Century (light blue). Red contours indicate the reference present-day ice sheet margin. Black dots indicate the six ice core locations.

https://doi.org/10.5194/egusphere-2026-6398
Preprint. Discussion started: 4 November 2026
© Author(s) 2026. CC BY 4.0 License.

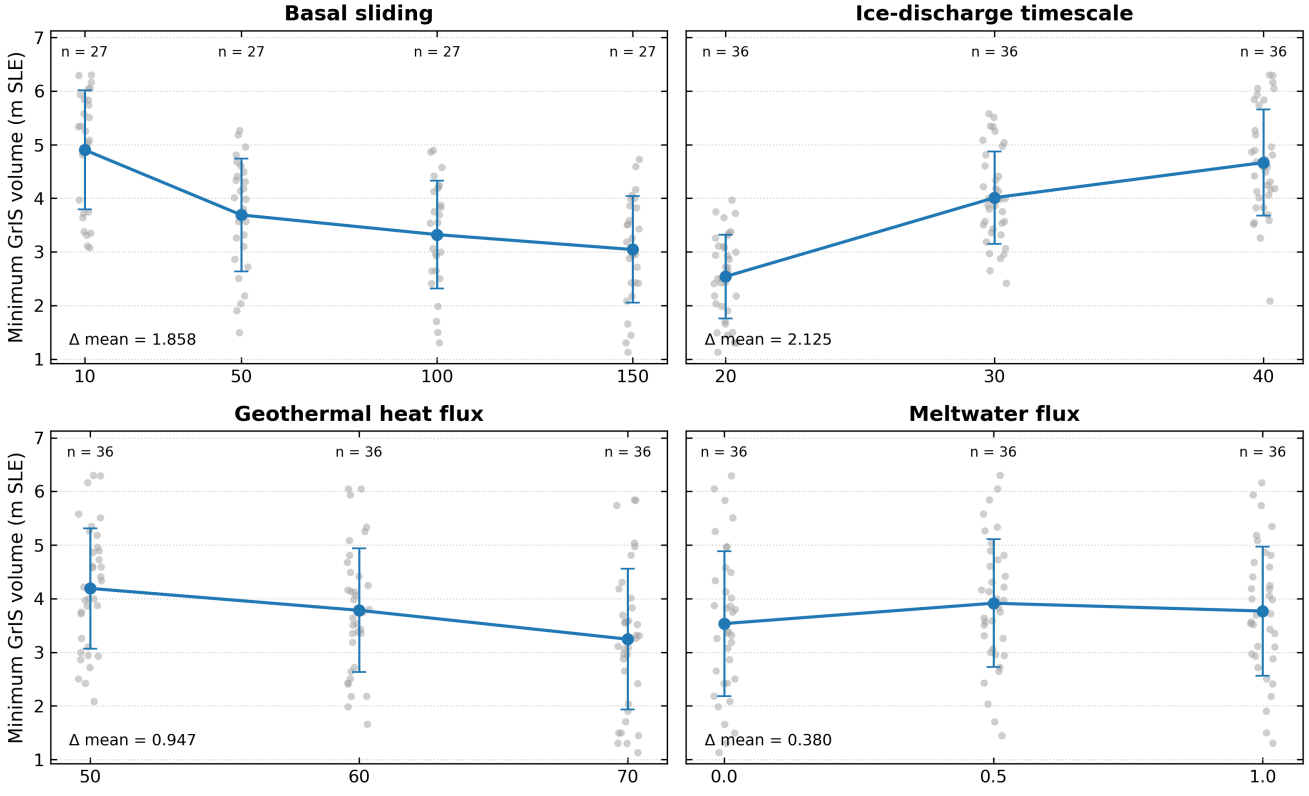


Figure A3. Single-parameter sensitivity analysis for each tested parameter and its effect on minimum Greenland Ice Sheet volume between 150–100 ka. Gray points represent individual simulations, while blue points indicuate the mean minimum ice volume for each parameter value. Error bars represent ±1 standard deviation. The number of simulations for each parameter is indicated by n and Δ mean represents the difference between the maximum and minimum parameter-level means, expressed in meters of sea level equivalent (m SLE).

https://doi.org/10.5194/egusphere-2026-6398
Preprint. Discussion started: 4 November 2026
© Author(s) 2026. CC BY 4.0 License.

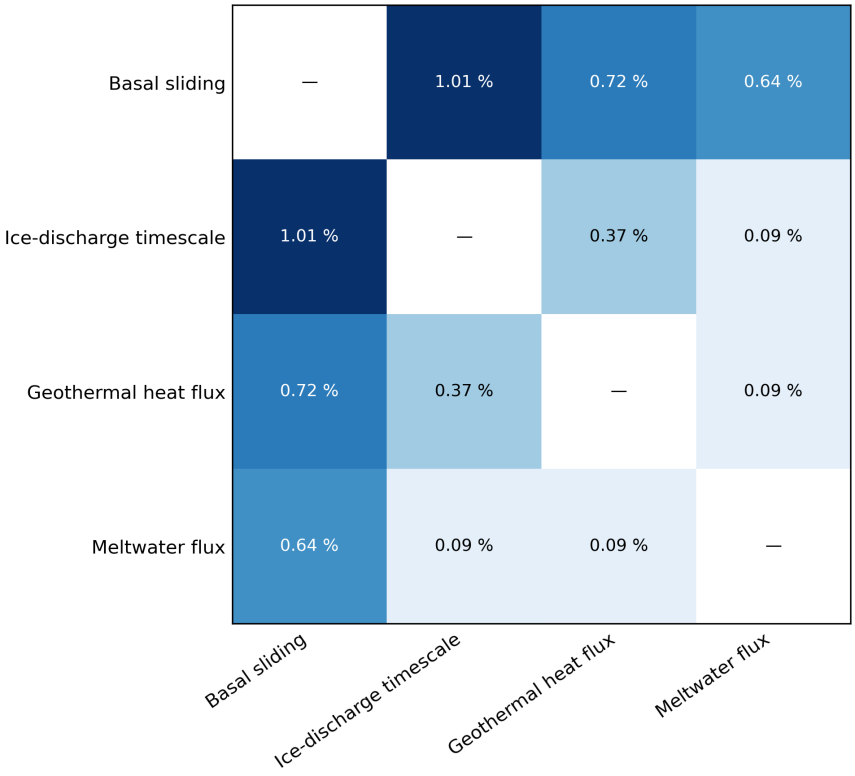


Figure A4. Contributions of two-way parameter interactions to the total variance in minimum Greenland Ice Sheet volume during 150–110 ka across the 108-member ensemble. Percentages indicate the proportion of total ensemble variance explained by each interaction. Darker shading represents greater contributions. Two-way interactions account for 2.9 % of the total variation.

https://doi.org/10.5194/egusphere-2026-6398
Preprint. Discussion started: 4 November 2026
© Author(s) 2026. CC BY 4.0 License.

Code and data availability. The source code of CLIMBER-X is available on Github (https://cxesmc.github.io/climber-x/), together with the input data and the instructions to install and run the model. The model output and derived datasets used in this study are available through Zenodo at https://doi.org/10.5281/zenodo.23483289 (Larson, 2026).

Author contributions. MM conceptualized the study. CL and MW designed the study. CL and MW tested and tuned various model parameters. CL ran the simulations, performed the analyses, and prepared the figures. CL wrote the manuscript, with contributions from all co-authors.

Competing interests. The authors declare that they have no competing interests.

Disclaimer. Publisher's note: Copernicus Publications remains neutral with regard to jurisdictional claims made in the text, published maps, institutional affiliations, or any other geographical representation in this paper. While Copernicus Publications makes every effort to include appropriate place names, the final responsibility lies with the authors. Views expressed in the text are those of the authors and do not necessarily reflect the views of the publisher.

Acknowledgements. The authors express deep gratitude for the Potsdam Institute for Climate Impact Research for providing the high-performance computer system used to perform the simulations. The authors also thank Alexander Robinson for his experimental framework and comments on this manuscript. This work was supported by funding from the University of Pennsylvania.

https://doi.org/10.5194/egusphere-2026-6398
Preprint. Discussion started: 4 November 2026
© Author(s) 2026. CC BY 4.0 License.

References

Alley, R. B., Andrews, J., Brigham-Grette, J., Clarke, G., Cuffey, K., Fitzpatrick, J., Funder, S., Marshall, S., Miller, G., Mitrovica, J., Muhs, D., Otto-Bliesner, B., Polyak, L., and White, J.: History of the Greenland Ice Sheet: paleoclimatic insights, Quaternary Science Reviews, 29, 1728–1756, https://doi.org/10.1016/j.quascirev.2010.02.007, 2010.

Aschwanden, A., Fahnestock, M. A., Truffer, M., Brinkerhoff, D. J., Hock, R., Khroulev, C., Mottram, R., and Khan, S. A.: Contribution of the Greenland Ice Sheet to sea level over the next millennium - SM, Science Advances, 5, eaav9396, https://doi.org/10.1126/sciadv.aav9396, 2019.

Bagge, M., Klemann, V., Steinberger, B., Latinović, M., and Thomas, M.: Glacial-Isostatic Adjustment Models Using Geodynamically Constrained 3D Earth Structures, Geochemistry, Geophysics, Geosystems, 22, e2021GC009 853, https://doi.org/10.1029/2021GC009853, 2021.

Bakker, P., Schmittner, A., Lenaerts, J. T. M., Abe-Ouchi, A., Bi, D., Van Den Broeke, M. R., Chan, W., Hu, A., Beadling, R. L., Marsland, S. J., Mernild, S. H., Saenko, O. A., Swingedouw, D., Sullivan, A., and Yin, J.: Fate of the Atlantic Meridional Overturning Circulation: Strong decline under continued warming and Greenland melting, Geophysical Research Letters, 43, https://doi.org/10.1002/2016GL070457, 2016.

Bender, M. L., Burgess, E., Alley, R. B., Barnett, B., and Clow, G. D.: On the nature of the dirty ice at the bottom of the GISP2 ice core, Earth and Planetary Science Letters, 299, 466–473, https://doi.org/10.1016/j.epsl.2010.09.033, 2010.

Bernales, J., Rogozhina, I., Greve, R., and Thomas, M.: Comparison of hybrid schemes for the combination of shallow approximations in numerical simulations of the Antarctic Ice Sheet, The Cryosphere, 11, 247–265, https://doi.org/10.5194/tc-11-247-2017, 2017.

Bonelli, S., Charbit, S., and Kageyama, M.: Investigating the evolution of major Northern Hemisphere ice sheets during the last glacial-interglacial cycle, Clim. Past, https://doi.org/10.5194/cp-5-329-2009, 2009.

Böning, C. W., Behrens, E., Biastoch, A., Getzlaff, K., and Bamber, J. L.: Emerging impact of Greenland meltwater on deepwater formation in the North Atlantic Ocean, Nature Geoscience, 9, 523–527, https://doi.org/10.1038/ngeo2740, 2016.

Calov, R., Ganopolski, A., Claussen, M., Petoukhov, V., and Greve, R.: Transient simulation of the last glacial inception. Part I: glacial inception as a bifurcation in the climate system, Climate Dynamics, 24, 545–561, https://doi.org/10.1007/s00382-005-0007-6, 2005.

Calov, R., Beyer, S., Greve, R., Beckmann, J., Willeit, M., Kleiner, T., Rückamp, M., Humbert, A., and Ganopolski, A.: Simulation of the future sea level contribution of Greenland with a new glacial system model, The Cryosphere, 12, 3097–3121, https://doi.org/10.5194/tc-12-3097-2018, 2018.

CAPE-Last Interglacial Project Members: Last Interglacial Arctic warmth confirms polar amplification of climate change, Quaternary Science Reviews, 25, 1383–1400, https://doi.org/10.1016/j.quascirev.2006.01.033, 2006.

Carrillo, J., Mann, M. E., Larson, C. J., Christiansen, S., Willeit, M., Ganopolski, A., Li, X., and Murphy, J. G.: Path-dependence of the Plio–Pleistocene glacial/interglacial cycles, Proceedings of the National Academy of Sciences, 121, e2322926 121, https://doi.org/10.1073/pnas.2322926121, 2024.

Christ, A. J., Bierman, P. R., Schaefer, J. M., Dahl-Jensen, D., Steffensen, J. P., Corbett, L. B., Peteet, D. M., Thomas, E. K., Steig, E. J., Rittenour, T. M., Tison, J.-L., Blard, P.-H., Perdrial, N., Dethier, D. P., Lini, A., Hidy, A. J., Caffee, M. W., and Southon, J.: A multimillion-year-old record of Greenland vegetation and glacial history preserved in sediment beneath 1.4 km of ice at Camp Century, Proceedings of the National Academy of Sciences, 118, e2021442 118, https://doi.org/10.1073/pnas.2021442118, 2021.

https://doi.org/10.5194/egusphere-2026-6398
Preprint. Discussion started: 4 November 2026
© Author(s) 2026. CC BY 4.0 License.

Christ, A. J., Rittenour, T. M., Bierman, P. R., Keisling, B. A., Knutz, P. C., Thomsen, T. B., Keulen, N., Fosdick, J. C., Hemming, S. R., Tison, J.-L., Blard, P.-H., Steffensen, J. P., Caffee, M. W., Corbett, L. B., Dahl-Jensen, D., Dethier, D. P., Hidy, A. J., Perdrial, N., Peteet, D. M., Steig, E. J., and Thomas, E. K.: Deglaciation of northwestern Greenland during Marine Isotope Stage 11, https://doi.org/10.1126/science.ade4248, 2023.

Clark, P. U. and Pollard, D.: Origin of the Middle Pleistocene Transition by ice sheet erosion of regolith, Paleoceanography, 13, 1–9, https://doi.org/10.1029/97PA02660, 1998.

Cuffey, K. M. and Marshall, S. J.: Substantial contribution to sea-level rise during the last interglacial from the Greenland ice sheet, Nature, 404, 591–594, https://doi.org/10.1038/35007053, 2000.

Dendy, S., Austermann, J., Creveling, J., and Mitrovica, J.: Sensitivity of Last Interglacial sea-level high stands to ice sheet configuration during Marine Isotope Stage 6, Quaternary Science Reviews, 171, 234–244, https://doi.org/10.1016/j.quascirev.2017.06.013, 2017.

Dutton, A., Carlson, A. E., Long, A. J., Milne, G. A., Clark, P. U., DeConto, R., Horton, B. P., Rahmstorf, S., and Raymo, M. E.: Sea-level rise due to polar ice-sheet mass loss during past warm periods, Science, 349, aaa4019, https://doi.org/10.1126/science.aaa4019, 2015.

Edwards, N. R. and Marsh, R.: Uncertainties due to transport-parameter sensitivity in an efficient 3-D ocean-climate model, Climate Dynamics, 24, 415–433, https://doi.org/10.1007/s00382-004-0508-8, 2005.

Edwards, N. R., Willmott, A. J., and Killworth, P. D.: On the Role of Topography and Wind Stress on the Stability of the Thermohaline Circulation, Journal of Physical Oceanography, 28, 756–778, https://doi.org/10.1175/1520-0485(1998)028<0756:OTROTA>2.0.CO;2, 1998.

Galaasen, E. V., Ninnemann, U. S., Irvalı, N., Kleiven, H. K. F., Rosenthal, Y., Kissel, C., and Hodell, D. A.: Rapid Reductions in North Atlantic Deep Water During the Peak of the Last Interglacial Period, Science, 343, 1129–1132, https://doi.org/10.1126/science.1248667, 2014.

Ganopolski, A. and Brovkin, V.: Simulation of climate, ice sheets and CO₂ evolution during the last four glacial cycles with an Earth system model of intermediate complexity, Climate of the Past, 13, 1695–1716, https://doi.org/10.5194/cp-13-1695-2017, 2017.

Ganopolski, A., Calov, R., and Claussen, M.: Simulation of the last glacial cycle with a coupled climate ice-sheet model of intermediate complexity, Clim. Past, https://doi.org/10.5194/cp-6-229-2010, 2010.

Goelzer, H., Huybrechts, P., Loutre, M.-F., and Fichefet, T.: Last Interglacial climate and sea-level evolution from a coupled ice sheet–climate model, Climate of the Past, 12, 2195–2213, https://doi.org/10.5194/cp-12-2195-2016, 2016.

Greve, R.: Application of a Polythermal Three-Dimensional Ice Sheet Model to the Greenland Ice Sheet: Response to Steady-State and Transient Climate Scenarios, Journal of Climate, 10, 901–918, https://doi.org/10.1175/1520-0442(1997)010<0901:AOAPTD>2.0.CO;2, 1997.

Greve, R. and Blatter, H.: Comparison of thermodynamics solvers in the polythermal ice sheet model SICOPOLIS, Polar Science, 10, 11–23, https://doi.org/10.1016/j.polar.2015.12.004, 2016.

Helsen, M. M., van de Berg, W. J., van de Wal, R. S. W., van den Broeke, M. R., and Oerlemans, J.: Coupled regional climate–ice-sheet simulation shows limited Greenland ice loss during the Eemian, Climate of the Past, 9, 1773–1788, https://doi.org/10.5194/cp-9-1773-2013, 2013.

Holschuh, N., Christianson, K., Dienstfrey, W., Hills, B., Hoffman, A. O., Paden, J., Winter, K., and Zuraw, R.: Entrained debris records regrowth of the Greenland Ice Sheet after the last interglacial, Nature Geoscience, 19, 573–580, https://doi.org/10.1038/s41561-026-01950-1, 2026.

https://doi.org/10.5194/egusphere-2026-6398
Preprint. Discussion started: 4 November 2026
© Author(s) 2026. CC BY 4.0 License.

Huybrechts, P.: Sea-level changes at the LGM from ice-dynamic reconstructions of the Greenland and Antarctic ice sheets during the glacial cycles, Quaternary Science Reviews, 21, 203–231, https://doi.org/10.1016/S0277-3791(01)00082-8, 2002.

Jiang, Z., Brierley, C., Thornalley, D., and Sax, S.: No changes in overall AMOC strength in interglacial PMIP4 time slices, Climate of the Past, 19, 107–121, https://doi.org/10.5194/cp-19-107-2023, 2023.

Klemann, V., Martinec, Z., and Ivins, E. R.: Glacial isostasy and plate motion, Journal of Geodynamics, 46, 95–103, https://doi.org/10.1016/j.jog.2008.04.005, 2008.

Kopp, R. E., Simons, F. J., Mitrovica, J. X., Maloof, A. C., and Oppenheimer, M.: Probabilistic assessment of sea level during the last interglacial stage, Nature, 462, 863–867, https://doi.org/10.1038/nature08686, 2009.

Köhler, P., Nehrbass-Ahles, C., Schmitt, J., Stocker, T. F., and Fischer, H.: Continuous record of the atmospheric greenhouse gas carbon dioxide (CO2), raw data, https://doi.org/10.1594/PANGAEA.871265, 2017.

Landais, A., Masson-Delmotte, V., Capron, E., Langebroek, P. M., Bakker, P., Stone, E. J., Merz, N., Raible, C. C., Fischer, H., Orsi, A., Prié, F., Vinther, B., and Dahl-Jensen, D.: How warm was Greenland during the last interglacial period?, Climate of the Past, 12, 1933–1948, https://doi.org/10.5194/cp-12-1933-2016, 2016.

Larour, E., Seroussi, H., Morlighem, M., and Rignot, E.: Continental scale, high order, high spatial resolution, ice sheet modeling using the Ice Sheet System Model (ISSM), Journal of Geophysical Research: Earth Surface, 117, 2011JF002 140, https://doi.org/10.1029/2011JF002140, 2012.

Larson, C.: CLIMBER-X Last Interglacial Greenland Ice Sheet ensemble: simulation results, https://doi.org/10.5281/zenodo.23483289, 2026.

Laskar, J., Fienga, A., Gastineau, M., and Manche, H.: La2010: a new orbital solution for the long-term motion of the Earth, Astronomy & Astrophysics, 532, A89, https://doi.org/10.1051/0004-6361/201116836, 2011.

Laske, G., Masters, G., Ma, Z., and Pasyanos, M.: Update on CRUST1.0 - A 1-degree Global Model of Earth's Crust, in: EGU General Assembly Conference Abstracts, EGU General Assembly Conference Abstracts, pp. EGU2013–2658, https://ui.adsabs.harvard.edu/abs/2013EGUGA..15.2658L, 2013.

Lhomme, N., Clarke, G. K., and Marshall, S. J.: Tracer transport in the Greenland Ice Sheet: constraints on ice cores and glacial history, Quaternary Science Reviews, 24, 173–194, https://doi.org/10.1016/j.quascirev.2004.08.020, 2005.

Lisiecki, L. E. and Raymo, M. E.: A Pliocene-Pleistocene stack of 57 globally distributed benthic δ^{18}O records: PLIOCENE-PLEISTOCENE BENTHIC STACK, Paleoceanography, 20, n/a–n/a, https://doi.org/10.1029/2004PA001071, 2005.

Loulergue, L., Schilt, A., Spahni, R., Masson-Delmotte, V., Blunier, T., Lemieux, B., Barnola, J.-M., Raynaud, D., Stocker, T. F., and Chappellaz, J.: Orbital and millennial-scale features of atmospheric CH4 over the past 800,000 years, Nature, 453, 383–386, https://doi.org/10.1038/nature06950, 2008.

Luo, Y., Tjiputra, J., Guo, C., Zhang, Z., and Lippold, J.: Atlantic deep water circulation during the last interglacial, Scientific Reports, 8, 4401, https://doi.org/10.1038/s41598-018-22534-z, 2018.

Lüthi, D., Le Floch, M., Bereiter, B., Blunier, T., Barnola, J.-M., Siegenthaler, U., Raynaud, D., Jouzel, J., Fischer, H., Kawamura, K., and Stocker, T. F.: High-resolution carbon dioxide concentration record 650,000–800,000 years before present, Nature, 453, 379–382, https://doi.org/10.1038/nature06949, 2008.

Ma, Q., Shi, X., Scholz, P., Sidorenko, D., Lohmann, G., and Ionita, M.: Revisiting climate impacts of an AMOC slowdown: dependence on freshwater locations in the North Atlantic, Science Advances, 10, eadr3243, https://doi.org/10.1126/sciadv.adr3243, 2024.

https://doi.org/10.5194/egusphere-2026-6398
Preprint. Discussion started: 4 November 2026
© Author(s) 2026. CC BY 4.0 License.

MacGregor, J. A., Fahnestock, M. A., Catania, G. A., Aschwanden, A., Clow, G. D., Colgan, W. T., Gogineni, S. P., Morlighem, M., Nowicki, S. M. J., Paden, J. D., Price, S. F., and Seroussi, H.: A synthesis of the basal thermal state of the Greenland Ice Sheet, Journal of Geophysical Research: Earth Surface, 121, 1328–1350, https://doi.org/10.1002/2015jf003803, 2016.

Martinec, Z., Klemann, V., van der Wal, W., Riva, R. E. M., Spada, G., Sun, Y., Melini, D., Kachuck, S. B., Barletta, V., Simon, K., A, G., and James, T. S.: A benchmark study of numerical implementations of the sea level equation in GIA modelling, Geophysical Journal International, 215, 389–414, https://doi.org/10.1093/gji/ggy280, 2018.

McKay, N. P., Overpeck, J. T., and Otto-Bliesner, B. L.: The role of ocean thermal expansion in Last Interglacial sea level rise: THERMAL EXPANSION IN LIG SEA LEVEL RISE, Geophysical Research Letters, 38, n/a–n/a, https://doi.org/10.1029/2011GL048280, 2011.

McManus, J. F., Francois, R., Gherardi, J.-M., Keigwin, L. D., and Brown-Leger, S.: Collapse and rapid resumption of Atlantic meridional circulation linked to deglacial climate changes, Nature, 428, 834–837, https://doi.org/10.1038/nature02494, 2004.

Morlighem, M., Williams, C. N., Rignot, E., An, L., Arndt, J. E., Bamber, J. L., Catania, G., Chauché, N., Dowdeswell, J. A., Dorschel, B., Fenty, I., Hogan, K., Howat, I., Hubbard, A., Jakobsson, M., Jordan, T. M., Kjeldsen, K. K., Millan, R., Mayer, L., Mouginot, J., Noël, B. P. Y., O'Cofaigh, C., Palmer, S., Rysgaard, S., Seroussi, H., Siegert, M. J., Slabon, P., Straneo, F., van den Broeke, M. R., Weinrebe, W., Wood, M., and Zinglersen, K. B.: BedMachine v3: Complete Bed Topography and Ocean Bathymetry Mapping of Greenland From Multibeam Echo Sounding Combined With Mass Conservation, Geophysical Research Letters, 44, https://doi.org/10.1002/2017GL074954, 2017.

Morlighem, M., Williams, C. N., Rignot, E., An, L., Arndt, J. E., Bamber, J. L., Catania, G., Chauché, N., Dowdeswell, J. A., Dorschel, B., Fenty, I., Hogan, K., Howat, I., Hubbard, A., Jakobsson, M., Jordan, T. M., Kjeldsen, K. K., Millan, R., Mayer, L., Mouginot, J., Noël, B. P. Y., O'Cofaigh, C., Palmer, S., Rysgaard, S., Seroussi, H., Siegert, M. J., Slabon, P., Straneo, F., Van Den Broeke, M. R., Weinrebe, W., Wood, M., and Zinglersen, K. B.: IceBridge BedMachine Greenland, Version 6, https://doi.org/10.5067/6B6B225B8V2D, 2025.

NEEM community members: Eemian interglacial reconstructed from a Greenland folded ice core, Nature, 493, 489–494, https://doi.org/10.1038/nature11789, 2013.

North Greenland Ice Core Project members: High-resolution record of Northern Hemisphere climate extending into the last interglacial period, Nature, 431, 147–151, https://doi.org/10.1038/nature02805, 2004.

Otto-Bliesner, B. L., Rosenbloom, N., Stone, E. J., McKay, N. P., Lunt, D. J., Brady, E. C., and Overpeck, J. T.: How warm was the last interglacial? New model–data comparisons, Philosophical Transactions of the Royal Society A: Mathematical, Physical and Engineering Sciences, 371, 20130 097, https://doi.org/10.1098/rsta.2013.0097, 2013.

Otto-Bliesner, B. L., Brady, E. C., Zhao, A., Brierley, C. M., Axford, Y., Capron, E., Govin, A., Hoffman, J. S., Isaacs, E., Kageyama, M., Scussolini, P., Tzedakis, P. C., Williams, C. J. R., Wolff, E., Abe-Ouchi, A., Braconnot, P., Ramos Buarque, S., Cao, J., De Vernal, A., Guarino, M. V., Guo, C., LeGrande, A. N., Lohmann, G., Meissner, K. J., Menviel, L., Morozova, P. A., Nisancioglu, K. H., O'ishi, R., Salas Y Mélia, D., Shi, X., Sicard, M., Sime, L., Stepanek, C., Tomas, R., Volodin, E., Yeung, N. K. H., Zhang, Q., Zhang, Z., and Zheng, W.: Large-scale features of Last Interglacial climate: results from evaluating the *lig127k* simulations for the Coupled Model Intercomparison Project (CMIP6)–Paleoclimate Modeling Intercomparison Project (PMIP4), Climate of the Past, 17, 63–94, https://doi.org/10.5194/cp-17-63-2021, 2021.

Plach, A., Nisancioglu, K. H., Langebroek, P. M., Born, A., and Le Clec'H, S.: Eemian Greenland ice sheet simulated with a higher-order model shows strong sensitivity to surface mass balance forcing, The Cryosphere, 13, 2133–2148, https://doi.org/10.5194/tc-13-2133-2019, 2019.

https://doi.org/10.5194/egusphere-2026-6398
Preprint. Discussion started: 4 November 2026
© Author(s) 2026. CC BY 4.0 License.

Quiquet, A. and Roche, D. M.: Investigating similarities and differences of the penultimate and last glacial terminations with a coupled ice sheet–climate model, Climate of the Past, 20, 1365–1385, https://doi.org/10.5194/cp-20-1365-2024, 2024.

Quiquet, A., Ritz, C., Punge, H. J., and Salas Y Mélia, D.: Greenland ice sheet contribution to sea level rise during the last interglacial period: a modelling study driven and constrained by ice core data, Climate of the Past, 9, 353–366, https://doi.org/10.5194/cp-9-353-2013, 2013.

Rainsley, E., Menviel, L., Fogwill, C. J., Turney, C. S. M., Hughes, A. L. C., and Rood, D. H.: Greenland ice mass loss during the Younger Dryas driven by Atlantic Meridional Overturning Circulation feedbacks, Scientific Reports, 8, 11 307, https://doi.org/10.1038/s41598-018-29226-8, 2018.

Raynaud, D., Chappellaz, J., Ritz, C., and Martinerie, P.: Air content along the Greenland Ice Core Project core: A record of surface climatic parameters and elevation in central Greenland, Journal of Geophysical Research: Oceans, 102, 26 607–26 613, https://doi.org/10.1029/97JC01908, 1997.

Reyes, A. V., Carlson, A. E., Beard, B. L., Hatfield, R. G., Stoner, J. S., Winsor, K., Welke, B., and Ullman, D. J.: South Greenland ice-sheet collapse during Marine Isotope Stage 11, Nature, 510, 525–528, https://doi.org/10.1038/nature13456, 2014.

Robinson, A., Calov, R., and Ganopolski, A.: Greenland ice sheet model parameters constrained using simulations of the Eemian Interglacial, Climate of the Past, 7, 381–396, https://doi.org/10.5194/cp-7-381-2011, 2011.

Robinson, A., Calov, R., and Ganopolski, A.: Multistability and critical thresholds of the Greenland ice sheet, Nature Climate Change, 2, 429–432, https://doi.org/10.1038/nclimate1449, 2012.

Robinson, A., Alvarez-Solas, J., Calov, R., Ganopolski, A., and Montoya, M.: MIS-11 duration key to disappearance of the Greenland ice sheet, Nature Communications, 8, 16 008, https://doi.org/10.1038/ncomms16008, 2017.

Schaefer, J. M., Finkel, R. C., Balco, G., Alley, R. B., Caffee, M. W., Briner, J. P., Young, N. E., Gow, A. J., and Schwartz, R.: Greenland was nearly ice-free for extended periods during the Pleistocene, Nature, 540, 252–255, https://doi.org/10.1038/nature20146, 2016.

Schilt, A., Baumgartner, M., Schwander, J., Buiron, D., Capron, E., Chappellaz, J., Loulergue, L., Schüpbach, S., Spahni, R., Fischer, H., and Stocker, T. F.: Atmospheric nitrous oxide during the last 140,000years, Earth and Planetary Science Letters, 300, 33–43, https://doi.org/10.1016/j.epsl.2010.09.027, 2010.

SICOPOLIS Authors: SICOPOLIS v5.3, https://doi.org/10.5281/zenodo.6872611, 2022.

Snyder, C. W.: Evolution of global temperature over the past two million years, Nature, 538, 226–228, https://doi.org/10.1038/nature19798, 2016.

Sommers, A. N., Otto-Bliesner, B. L., Lipscomb, W. H., Lofverstrom, M., Shafer, S. L., Bartlein, P. J., Brady, E. C., Kluzek, E., Leguy, G., Thayer-Calder, K., and Tomas, R. A.: Retreat and Regrowth of the Greenland Ice Sheet During the Last Interglacial as Simulated by the CESM2-CISM2 Coupled Climate–Ice Sheet Model, Paleoceanography and Paleoclimatology, 36, e2021PA004 272, https://doi.org/10.1029/2021PA004272, 2021.

Spratt, R. M. and Lisiecki, L. E.: A Late Pleistocene sea level stack, Climate of the Past, 12, 1079–1092, https://doi.org/10.5194/cp-12-1079-2016, 2016.

Stone, E. J., Lunt, D. J., Annan, J. D., and Hargreaves, J. C.: Quantification of the Greenland ice sheet contribution to Last Interglacial sea level rise, Climate of the Past, 9, 621–639, https://doi.org/10.5194/cp-9-621-2013, 2013.

Tarasov, L. and Peltier, W. R.: Greenland glacial history, borehole constraints, and Eemian extent, Journal of Geophysical Research: Solid Earth, 108, 2001JB001 731, https://doi.org/10.1029/2001JB001731, 2003.

Van Westen, R. M., Vanderborght, E., Kliphuis, M., and Dijkstra, H. A.: Physics-Based Indicators for the Onset of an AMOC Collapse Under Climate Change, Journal of Geophysical Research: Oceans, 130, e2025JC022 651, https://doi.org/10.1029/2025JC022651, 2025.

https://doi.org/10.5194/egusphere-2026-6398
Preprint. Discussion started: 4 November 2026
© Author(s) 2026. CC BY 4.0 License.

Willeit, M. and Ganopolski, A.: PALADYN v1.0, a comprehensive land surface–vegetation–carbon cycle model of intermediate complexity, Geoscientific Model Development, 9, 3817–3857, https://doi.org/10.5194/gmd-9-3817-2016, 2016.

Willeit, M., Ganopolski, A., Calov, R., and Brovkin, V.: Mid-Pleistocene transition in glacial cycles explained by declining CO2 and regolith removal, SCIENCE ADVANCES, p. 9, https://doi.org/10.1126/sciadv.aav7337, 2019.

Willeit, M., Ganopolski, A., Robinson, A., and Edwards, N. R.: The Earth system model CLIMBER-X v1.0 – Part 1: Climate model description and validation, Geoscientific Model Development, 15, 5905–5948, https://doi.org/10.5194/gmd-15-5905-2022, 2022.

Willeit, M., Calov, R., Talento, S., Greve, R., Bernales, J., Klemann, V., Bagge, M., and Ganopolski, A.: Glacial inception through rapid ice area increase driven by albedo and vegetation feedbacks, Climate of the Past, 20, 597–623, https://doi.org/10.5194/cp-20-597-2024, 2024.

Willerslev, E., Cappellini, E., Boomsma, W., Nielsen, R., Hebsgaard, M. B., Brand, T. B., Hofreiter, M., Bunce, M., Poinar, H. N., Dahl-Jensen, D., Johnsen, S., Steffensen, J. P., Bennike, O., Schwenninger, J.-L., Nathan, R., Armitage, S., De Hoog, C.-J., Alfimov, V., Christl, M., Beer, J., Muscheler, R., Barker, J., Sharp, M., Penkman, K. E. H., Haile, J., Taberlet, P., Gilbert, M. T. P., Casoli, A., Campani, E., and Collins, M. J.: Ancient Biomolecules from Deep Ice Cores Reveal a Forested Southern Greenland, Science, 317, 111–114, https://doi.org/10.1126/science.1141758, 2007.

Wunderling, N., Von Der Heydt, A. S., Aksenov, Y., Barker, S., Bastiaansen, R., Brovkin, V., Brunetti, M., Couplet, V., Kleinen, T., Lear, C. H., Lohmann, J., Roman-Cuesta, R. M., Sinet, S., Swingedouw, D., Winkelmann, R., Anand, P., Barichivich, J., Bathiany, S., Baudena, M., Bruun, J. T., Chiessi, C. M., Coxall, H. K., Docquier, D., Donges, J. F., Falkena, S. K. J., Klose, A. K., Obura, D., Rocha, J., Rynders, S., Steinert, N. J., and Willeit, M.: Climate tipping point interactions and cascades: a review, Earth System Dynamics, 15, 41–74, https://doi.org/10.5194/esd-15-41-2024, 2024.

Yau, A. M., Bender, M. L., Blunier, T., and Jouzel, J.: Setting a chronology for the basal ice at Dye-3 and GRIP: Implications for the long-term stability of the Greenland Ice Sheet, Earth and Planetary Science Letters, 451, 1–9, https://doi.org/10.1016/j.epsl.2016.06.053, 2016a.

Yau, A. M., Bender, M. L., Robinson, A., and Brook, E. J.: Reconstructing the last interglacial at Summit, Greenland: Insights from GISP2, Proceedings of the National Academy of Sciences, 113, 9710–9715, https://doi.org/10.1073/pnas.1524766113, 2016b.

Zhang, R., Sutton, R., Danabasoglu, G., Kwon, Y., Marsh, R., Yeager, S. G., Amrhein, D. E., and Little, C. M.: A Review of the Role of the Atlantic Meridional Overturning Circulation in Atlantic Multidecadal Variability and Associated Climate Impacts, Reviews of Geophysics, 57, 316–375, https://doi.org/10.1029/2019RG000644, 2019.

Zhang, T., Colgan, W., Wansing, A., Løkkegaard, A., Leguy, G., Lipscomb, W. H., and Xiao, C.: Evaluating different geothermal heat-flow maps as basal boundary conditions during spin-up of the Greenland ice sheet, The Cryosphere, 18, 387–402, https://doi.org/10.5194/tc-18-387-2024, 2024.